U.PORTO

MESTRADO ONCOLOGIA

ONCOLOGIA LABORATORIAL

The origin of tumour-infiltrating regulatory T cells

João Augusto Freitas

M

2019

U.PORTO

João Augusto Freitas. The origin of tumour-infiltrating regulatory T cells

The origin of tumour-infiltrating regulatory T cells

João Augusto Teixeira de Freitas

INSTITUTO DE CIÊNCIAS BIOMÉDICAS ABEL SALAZAR

M.ICBAS 2019

João Augusto Teixeira de Freitas

The origin of tumour-infiltrating regulatory T cells

Dissertação de Candidatura ao grau de Mestre em Oncologia- Especialização em Oncologia laboratorial submetida ao Instituto de Ciências Biomédicas Abel Salazar da Universidade do Porto

Orientador- Professor Doutor José Carlos Lemos Machado
Categoria- Professor associado e investigador principal
Afiliação- Faculdade de Medicina da Universidade do Porto (FMUP), Instituto Patologia e Imunologia Molecular da Universidade do Porto (IPATIMUP) e Instituto de Investigação e Inovação em Saúde (i3s)

Co-orientador- Doutora Carla Marina Pereira Gomes
Categoria- Junior Researcher
Afiliação- Instituto de Investigação e Inovação em Saúde (i3s) e Instituto de Patologia e Imunologia Molecular da Universidade do Porto (IPATIMUP)

Acknowledgements

Muitas foram as pessoas, que possivelmente não irei mencionar aqui, mas que me ajudaram ao longo deste caminho. A todos esses o meu muito obrigado.

Primeiro, tenho de agradecer ao Professor Doutor José Carlos Machado por tão amavelmente ter me recebido no seu grupo de investigação e por ter acreditado em mim num projeto tão ambicioso e por ter me dado sempre as melhores condições para a execução desta dissertação.

Em segundo, tenho de agradecer à Doutora Carla Gomes por toda a passagem de sabedoria e tempo despendido em todas as minhas dúvidas e correções desta dissertação e sempre disponível para ajudar-me a ultrapassar os problemas.

Também gostaria de destacar três pessoas muito importantes neste percurso e que não podia passar sem agradecer, ao Carlos Resende e ao professor José Luís Costa, por todos os conselhos e ajuda que me deu ao longo deste ano e à Helena Ferreira, por ter sido a pessoa que me ensinou muito do que sei hoje, e pela sua paciência para me responder às perguntas quando eu tinha dúvidas existenciais.

Também este trabalho não teria sido conseguido se não tivesse tido o apoio durante este árduo ano dos Gedys, em especial da Susana, do Nuno, do João, da Ana Rita e da Joana Reis que de uma maneira ou de outras alegraram-me os dias e deram me sempre apoio nos bons e nos maus momentos e aconselharam me sempre que possível.

Também tenho de agradecer aos meus colegas de mestrado principalmente à alentejana, Silvana, Vera e Ana Marta pelos convívios, pelos passeios e pelos lanches que nos fazem esquecer o trabalho e que nos animam fazendo nos rir nos momentos que mais precisamos.

Uma palavra especial à Mafalda por ter tentado sempre me ajudar em tudo o que podia e não podia e com muita paciência para escutar me principalmente nos dias de frustração e dar sempre uma opinião/ideia para ultrapassar os problemas.

Por último mas não menos importante este trabalho não era possível sem o grande apoio da minha família, principalmente os meus pais que apesar de estarem do outro lado do atlântico sempre tentaram me proporcionar o melhor e estando sempre presentes nos momentos mais importantes mas também sempre preocupados quando estava mais em baixo, por isso esta tese é dedicada a eles e pelo seu enorme carinho e amor por estes anos todos.

Abbreviations and Symbols

AIRE- Autoimmune regulator
APC cy7- Allophycocyanin-Cyanine-7
Apc- Adenomatous polyposis coli
APC- Allophycocyanin
B6 mouse- C57BL/6 mouse
BAC- Bacterial artificial chromosome
C region- Constant region
CD- Cluster of differentiation
$CD4^+$ effector T cells- $CD4^+$ T_{eff} cells
cDNA- Complementary DNA
CDR- Complementary determining region
Cre- Cre recombinase
CTLA-4- Cytotoxic T-lymphocyte-associated protein 4
D region- Diversity region
DC- Dendritic cells
DGAV- Direção Geral de Alimentação e Veterinária
DNA- Deoxyribonucleic acid
DTR- Diphtheria toxin receptor
EGFP- Enhanced green fluorescent protein
ERT2- Estrogen receptor
FACS- Fluorescence activated cell sorting
FBS- Fetal bovine serum
FITC- Fluorescein isothiocyanate
Flox- Floxed
FoxP3- Forkhead box P3 factor
FSC-A- Forward scatter channel-area
FSC-H- Forward scatter channel-height
GI tract- Gastrointestinal tract
GITR- Glucocorticoid-induced TNFR-related gene
ICOS- Inducible T cell costimulatory
IFN γ- Interferon-gamma
IHC- Immunohistochemistry
IL- Interleukin
IPEX- Immune dysregulation, polyendocrinopathy, enteropathy, X-linked

J region- Joining region

LAG-3- Lymphocyte-activation gene 3

Lrig- Leucine-rich repeats and immunoglobulin-like domains 1

Luci- Luciferase

MDSC- Myeloid-derived suppressor cell

MHC- Major histocompatibility complex

Min- Minutes

NGS- Next-generation sequencing

NH_4cl- Ammonium chloride

Nk- Natural killer

NKT- Natural killer T

NRP1- Neuropilin-1

PBS- Phosphate buffer saline

PBS-T- PBS tween solution

PCR- Polymerase chain reaction

PD-1- Programmed cell death-1

PD-L1- Programmed death-ligand 1

PeCy7- Phycoerythrin-Cyanine-7

PercP- Peridinin chlorophyll

pTregs- Peripheral Tregs

Rag2- Recombination activating 2

RIN- RNA integrity number

RNA- Ribonucleic acid

Rpm- Rotations per minute

RPMI- Roswell Park Memorial Institute medium

RT- Room temperature

SSC-A- Side scatter channel- area

TCR- T cell receptor

TGF-β- Tumour growth factor β

Th- T helper

tiTreg- Tumour-infiltrating Treg

Tregs- Regulatory T cells

Tris-HCL- Tris hydrochloride

tTregs- Thymus-derived Tregs

V region- Variable region

Resumo

Atualmente, está bem documentado o duplo papel do sistema imunitário no desenvolvimento do cancro, que se por um lado contribuindo para a eliminação do tumor, por outro, pode promover a sua progressão. A tolerância imunitária é um dos processos descritos que permitem ao tumor escapar da resposta imunitária. Uma das principais vias envolvidas nesta tolerância atua através das células T reguladoras (Treg), caraterizadas pela expressão do factor de transcrição Forkhead box P3 (FoxP3). Estas células são uma subpopulação das células T $CD4^+$ e possuem uma função imunossupressora que é fundamental para a manutenção da tolerância imunológica. Esta população de células é frequentemente observada no cancro, contribuindo para um microambiente tumoral imunossupressor e favorecendo a progressão tumoral. De facto, a presença de Tregs no infiltrado tumoral tem sido associada a um mau prognóstico da doença, apesar de não haver concordância entre diferentes estudos e de dados recentes sugerirem que esse prognóstico pode variar dependo do tipo de cancro. Apesar disto, até ao momento, ainda não foram elucidados os mecanismos de recrutamento e atividade das células Tregs no contexto tumoral. Além disso, ainda não é conhecido se as Tregs presentes no tumour são provenientes do timo (tTreg) ou provenientes da conversão a partir de células T $CD4^+$ na periferia (pTreg).

Assim, o objetivo desta dissertação é o de identificar a origem das Tregs presentes no tumor.

Para tal, foram usados dois modelos animais de tumorigénese, os murganhos $Lrig1^{CreERT2/+}$;$Apc^{flox/+}$, que constituem um modelo de desenvolvimento de tumores induzíveis no intestino e colon, e murganhos $FoxP3^{eGFP.DTR.Luci}$, que apresentam todas as Tregs marcadas com uma proteína de fluorescência verde e nos quais desenvolveram tumores pela inoculação subcutânea de células tumorais MC38. Após obter uma suspensão de células proveniente de amostras de tumor e de sangue, estas foram caracterizadas em termos de composição imunológica por citometria de fluxo através do uso dos marcadores CD3, CD4, CD25 e FoxP3. As populações de linfócitos T efectores $CD4^+$ ($CD3^+CD4^+FoxP3^-$) e Tregs ($CD3^+CD4^+CD25^+FoxP3^+$) foram isoladas e, posteriormente, a cadeia β do recetor das células T (TCRβ) presente em cada população foi sequenciada pela técnica de sequenciação de nova geração (NGS). Por fim, os dados provenientes da sequenciação foram analisados e comparados entre as populações referidas anteriormente.

A presença de Tregs no tumor foi observada em ambos os modelos animais. De seguida foram realizadas comparações entre o repertório de TCRβ nas Tregs e nos linfócitos T

efectores $CD4^+$ dos tumores, indicando que a maioria das sequências não eram partilhadas entre estas populações. Desta forma, é possível concluir que a maioria dos clones de Tregs presentes no tumores eram de origem central. Apesar disso existe uma grande quantidade de clones de pTregs no tumor subcutâneo vindo do ratinho $FoxP3^{eGFP.DTR.Luci}$. Foi também efetuada uma comparação entre as populações de interesse presentes no tumor do ratinho $Lrig1^{CreERT2/+}$;$Apc^{flox/+}$ com as populações que circulavam no sangue, mostrando que alguns clones de Tregs periféricas são originadas no local do tumor, uma vez que apenas existe partilha entre as sequências de TCR das populações $CD4^+$ T efectoras e Tregs presentes nas amostras do tumorais.

Resumindo, o trabalho descrito nesta dissertação mostra que, em ambos os modelos animais, a maioria das clones de Tregs infiltradas no tumor parecem ter uma origem tímica apesar de também existir uma percentagem de Tregs convertidas na periferia e ambas desempenharem um papel fundamental no desenvolvimento de uma tolerância central e periférica, contribuindo para desvendar a sua implicação no processo de evasão imunológica no cancro.

Abstract

Nowadays, it is well established that the immune system plays a dual role in cancer development, either by contributing to tumour elimination or by promoting its progression. Immunotolerance is one of the processes which may allow tumour escape from the immune response. One of the main players of immunotolerance are regulatory T cells (Tregs), which are characterized by the expression of the Forkhead box P3 (FoxP3) transcription factor. Tregs are a subset of $CD4^+$ T cells with an immunosuppressive function that are fundamental in maintaining immunological tolerance. They are often observed in cancer, where they are thought to impose an immunosuppressive microenvironment that favours tumour progression. Indeed, the presence of tumour-infiltrating Tregs (tiTregs) is associated with poor prognosis, although there is some discrepant data suggesting that the prognostic value of tiTregs might vary according to the cancer type. Despite this, the mechanisms that govern the recruitment and activity of tiTregs are still poorly understood. Moreover, to date it has not yet been elucidated if these cells derive from thymic (central) selection of Tregs (tTregs), or whether tiTregs derive from the peripheral conversion of $CD4^+$ T_{effs} (pTregs). Therefore, the aim of this dissertation is to determine the origin of tiTregs.

We used two murine models of cancer, the $Lrig1^{CreERT2/+}$;$Apc^{flox/+}$ mice, which constitutes an inducible model of intestinal/colonic tumourigenesis, and the $FoxP3^{eGFP.DTR.Luci}$ mice, in which all Tregs are identified with a green fluorescent protein and where tumours were induced by subcutaneous inoculation of MC38 cells. After achieving a cell suspension from tumour and blood samples, immunophenotyping based on CD3, CD4, CD25 and FoxP3 markers were performed by flow cytometry to sort $CD4^+$ T_{eff} cells ($CD3^+CD4^+FoxP3^-$) and Tregs ($CD3^+CD4^+CD25^+FoxP3^+$) followed by T cell receptor β chain (TCRβ) sequencing for each population by Next Generation Sequencing (NGS). Finally, the sequencing data was analysed and compared between the $CD4^+$ T_{eff} and Tregs populations.

The presence of Tregs in the tumour site was observed in both models. Moreover, the comparison between the TCRβ repertoire of tumour-infiltrating Tregs and $CD4^+$ T_{eff} cells indicated that the majority of TCRβ sequences were not shared by these populations, concluding that the majority of tiTreg clones have a central origin. But in the case of MC38 derived subcutaneous tumour there is a substantial fraction of pTregs among tiTregs. We also compared the TCRβ sequences of $CD4^+$ T_{eff} and Tregs sorted from blood with the ones sorted from $Lrig1^{CreERT2/+}$;$Apc^{flox/+}$ tumour samples, and the obtained data revealed that at least some pTreg clones are converted from $CD4^+$ T_{eff} cells locally, at the tumour site.

In summary, the work described in this dissertation shows that, in both mouse models, tiTreg clonotypes appear to originate mostly from the thymus but also a few pTregs

clonotypes were present in tumour, hinting at a role for central and peripheral tolerance in tumour immune escape.

INDEX

List of figures

List of Tables

1. Introduction

1.1. The immune system and cancer

The impact of the immune system in cancer progression has been discussed by the scientific community for over a century [1]. In the early 20th century, Paul Ehlrich hypothesized that the immune system could control cancer development. However, this was not proven due to lack of knowledge about the composition and function of all immune system components, as well as insufficient experimental tools at the time [2]. Later on, some researchers demonstrated the stimulation of the immune system by tumour antigens and studies using mice showed that these can become resistant to syngeneic transplantable tumours induced by chemical and biological carcinogens, corroborating Paul Ehlrich's hypothesis [3, 4]. These findings were the basis for the "cancer immunosurveillance" hypothesis.

1.1.1. From cancer immunosurveillance to cancer immunoediting

The "cancer immunosurveillance" hypothesis was officially proposed by Burnet and Thomas in the mid 70's, after the discovery of the ability of antigen-presenting cells (APCs) to present tumour neo-antigens to immune cells and generate immune-related effector/memory cells [2, 5]. This theory supports the capacity of the adaptive immunity to prevent tumour formation, with lymphocytes having a leading role in the recognition and elimination of tumour cells [6].

However, studies showed another perspective of this hypothesis when comparing immunocompetent to "immunodeficient" mice [1]. In a study conducted by Stutman, researchers used nude mice as an immunodeficient model, but these animals show the presence of a small amount of adaptive immune cells, such as lymphocytes, and therefore, were not fully immunodeficient as previously thought [1, 7]. Thus, the results observed by Stutman showed no significant difference between "immunodeficient" and immunocompetent animals in terms of spontaneous tumour incidence, including in groups with different characteristics, such as the age of animals or the dose of carcinogens [7, 8]. As a result, it was argued that these tumour cells did not express enough antigens or they could not trigger an immune response, not being recognized by the immune system as non-self. Other authors defended that tumour cells are very similar to "normal cells", inducing the immune system to tolerate them [1, 9]. These new experiments and opinions led to the fall of the immunosurveillance concept [1].

In the 90s, immunodeficient animal models were improved. One of the major contributions to that was the discovery of the importance of interferon γ (IFNγ) in promoting immunologically induced rejection of transplanted tumour cells [1]. Another important contribution was the discovery of *Recombination activating 2 (Rag2)* gene that was found as an important gene in T cell receptor (TCR) and B cell receptor (BCR) rearrangement, being crucial for the development of T cells, natural killer T (NKT) cells and B cells [10]. Therefore, if the *IFNγ* gene or other gene involved in adaptive immunity, such as *Rag2*, were knocked out, these mice would be more susceptible to the development of spontaneous tumours, as well as carcinogen-induced tumours [1, 9]. According to Shankaran *et al*., tumours from different animals show different degrees of immunogenicity; therefore, the immune system can control tumour development but at the same time shape the tumour through the selection of less immunogenic clones [11].

Because immunosurveillance only referred the relationship between the immune system response and tumour elimination, a new concept emerged at this time: cancer immunoediting [2].

1.1.2. Cancer immunoediting

The hypothesis of cancer immunoediting, which stresses the dual role of the immune system in protecting the host and promoting tumour development, was proposed by Dunn and Schreiber, in 2002 [9]. According to these authors, cancer immunoediting proceeds sequentially in three different phases: elimination, equilibrium and escape, also known as the three E´s (Figure 1) [12]. However, in some cases, tumour cells may directly enter into either the equilibrium or escape phases without passing through an earlier stage [1]. Nowadays, this is the most accepted theory in the scientific community regarding the tumour sculpting actions of the immune system.

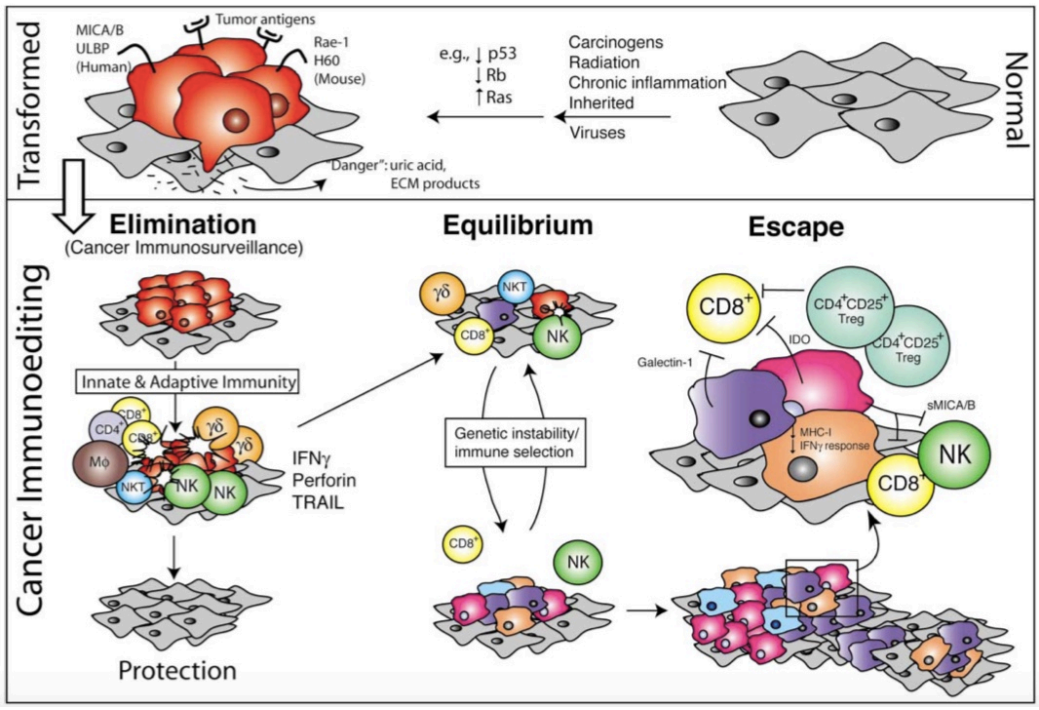

Figure 1. Cancer immunoediting hypothesis**.** Normal cells (in grey) are transformed into tumour cells (in red) by the action of some carcinogens, promoting their proliferation/survival (top side). After reaching this stage, tumours express tumour specific markers and their growth generate a pro-inflammatory signal of recruitment of both innate and adaptive immune cells to the tumour site (elimination phase). These recruited cells may eliminate the tumour and, thus, protect the host. Still, if the elimination of the tumour is not totally complete, a few of the tumour cell variants may survive and enter in a new phase (equilibrium), where they may be maintained chronically without evidence of growth or some resistant cells could emerge by alteration of constitution of tumour cell variants by the immune response and go through the next stage (escape), where the immune system is no longer able to eliminate tumour cells and the tumour will become clinically detectable. Reprinted from [13].

1.1.2.1. Elimination phase

The elimination phase is described as an updated version of the cancer immunosurveillance hypothesis, in which the innate and adaptive immune systems work together to detect and eliminate cancer cells [1, 14]. If it functions properly, the tumour is eliminated [9].

When tumours reach a certain size, they require an enhanced blood supply to initiate invasion. This growth triggers the expression of inflammatory signals, leading to the recruitment of innate immune cells, such as macrophages, natural killer (NK) cells and dendritic cells to the tumour site [12]. Some infiltrating lymphocytes like NKT cells and γδ T cells also recognise tumour cells and produce IFNγ, which induces anti-proliferative, apoptotic and angiostatic effects [15]. This inflammatory process leads to the recruitment of more NK cells and macrophages to the tumour site, followed by the transactivation of macrophages and NK cells through the production of IFNγ and interleukin-12 (IL-12) and elimination of tumour cells by secretion of tumour necrosis factor-related apoptosis-inducing ligand (TRAIL), perforin and reactive oxygen species (ROS) [9, 12].

Tumour cell fragments are then phagocytized by dendritic cells, which move to draining lymph nodes, where they present the antigens to $CD4^+$ T helper cells that will produce IFNγ

and induce the development of tumour specific $CD8^+$ T cells [1, 9, 12]. Finally, these cytotoxic T lymphocytes migrate to the tumour site and destroy the remaining tumour cells, whose immunogenicity had been enhanced by IFNγ [9].

1.1.2.2 Equilibrium phase

Even though the immune system eliminates most tumour cells in the elimination phase, minor tumour cell variants may survive and progress to the next stage, the equilibrium phase [1]. This is usually the longest phase of the immunoediting process and can last up to several years [12]. In equilibrium, the immune system maintains a residual tumour cell pool in a functional state of dormancy, a term used to describe latent tumour cells that may reside in patients for decades without tumour development, but will eventually resume growth as either recurrent primary tumours or distant metastases [1]. This occurs due to the presence of lymphocytes and IFNγ that continue on destroying different tumour cell clones [9]. More specifically, a high proportion of $CD8^+$ T cells, NK and $\gamma\delta$ T cells, and low proportions of NKT cells, regulatory T cells (Treg) and myeloid-derived suppressor cells (MDSC), allowing the presence of residual tumour [15, 16]. Furthermore, a study by Kobel suggests that only adaptive immunity is responsible for maintaining the equilibrium phase, which contrasts with the elimination phase [17].

1.1.2.3 Escape phase

In the last phase of the immunoediting process, the escape phase, the tumour cells that have acquired the ability to bypass the immune system recognition emerge as a progressively growing, clinically detectable tumour. This progression may occur due to selection by the immune system of tumour variants that are fitter to thrive and/or cancer-induced immunosuppression [1]. Still, several scientific groups are trying to better understand the molecular mechanisms underlying tumour immune escape, including downregulation/loss of tumour antigen expression or increased resistance to cytotoxic immunity effects, resulting in poorly immunogenic tumour cells [1, 15]. Besides that, tumour cells can produce immune suppressive cytokines, such as tumour growth factor β (TGF-β), express negative immune checkpoints like programmed death-ligand 1 (PD-L1) or recruit suppressor immune cells, such as Treg cells or MDSC to promote a tumour microenvironment that favours the escape from the immune system [1, 14].

1.2. Immunotherapy: a new approach for cancer treatment

With growing evidence regarding the importance of the immune system in cancer development, a new paradigm for cancer patients treatment has emerged: cancer immunotherapy [18]. In this type of treatment, the focus is on the immune system rather than the tumour cells, which are the conventional target for traditional forms of treatment like chemotherapy or target therapies, such as tyrosine kinase inhibitors [19]. In this new approach, the treatment activates the immune system to fight cancer, mimicking what happens in the elimination phase of the immunoediting hypothesis. To achieve this, several studies focus on obtaining an effective T cell response, especially by removing the "brake" of $CD8^+$ cytotoxic T cells, thereafter, eliminating the tumour. One of the new strategies to activate $CD8^+$ cytotoxic T cells is the administration of immune checkpoint blockade molecules such as anti-PD-L1/programmed cell death-1 (PD-1) and anti-cytotoxic T-lymphocyte-associated protein 4 (CTLA-4) [20]. Despite the initial favourable results in the clinics for inhibitors of these molecules, they have only been approved for a reduced number of types of cancer, such as melanoma and non-small cell lung cancer, by the Food and Drug Administration (FDA) agency, in the USA [21]. Moreover, only a subgroup of about 20-30% of treated patients have benefited from this treatment [22]. There are many factors contributing to that result: firstly, some patients had primary resistance to the treatment; secondly, due to dysregulation of the immune response by these immune checkpoint inhibitors, some patients have developed severe adverse effects and others have relapsed after a few months/years, despite presenting a good initial response [23].

For these reasons, it is important to explore and target other pathways that are not directly related to the activation of intrinsic $CD8^+$ cytotoxic T cells, but through which tumour cells can escape from the immune response. New immunotherapeutic drugs may be used alone or in combination with current immunotherapy or traditional therapies, and in a wider range of patients that will benefit from increased overall survival [19, 24].

1.3. T cell development

Since research of immunotherapeutic drugs is mainly focused on T cells, it is essential to comprehend more about T cell development. Contrary to what occurs with other immune cells, where all stages of development occur in the bone marrow, the primary lymphoid organ for T cell maturation is the thymus [25]. Besides, T cells have a unique marker, the TCR, which is a key element in T cell activation and is also assembled in the thymus [26].

Initially, T cell precursors enter the thymus and go to the cortex region. There, these cells, also known as thymocytes, present a double negative (DN) phenotype, since neither CD4 or CD8 markers are expressed [27, 28]. This pool of cells includes both $\alpha\beta$T and $\gamma\delta$T cells.

About 90% to 99% of T cells have the αβTCR and they need two steps to form the TCR protein [29]. Firstly, the TCRβ, also known as TRB, is rearranged and, only in cells in which it is assembled correctly, the TCRα is formed [27]. The *TCRβ* gene is composed of one constant region (C) and three different variable regions: variable (V region), diversity (D region) and joining (J region), each comprising several segments (Table 1). The *TCRα* gene is relatively similar to the *TCRβ* gene, despite having only two different variable regions, V and J [29].

Regarding the TCR protein, it can be divided in three parts, based on structural folds: complementary determining region (CDR) 1, CDR2 (encoded by the V region) and CDR3 (encoded by the end of the V region, the entire D region and the 5´ portion of J region). Due to the inclusion of all the junctional diversity, CDR3 is the most diverse region, which is of extreme importance as it is the region that recognizes antigenic peptides [29, 30].

Before TCR protein assembly, it is necessary to have a recombination in the DNA strain regions referred. First, a couple of nucleases, Rag1 and Rag2, recognise one specific sequence in two random segments from different regions (V-J) and cleaves those locations. This sequence is present in the beginning and/or end of each segment of the V, D and J regions. After the DNA strains are cut, random nucleotides are added to both strains by terminal deoxynucleotide transferase (TdT). Finally, a complex of enzymes align both strains of DNA and ligate the two segments (Figure 2A) [31, 32]. In the case of the TCRβ chain, it is necessary to recombine first the D-J and then the V -DJ regions (Figure 2B) [32]. Due to the random recombination in each segment of the different regions, as well as to the introduction of new random nucleotides by TdT enzymes, virtually every T cell will have a different TCR sequence. The estimated number of possible different TCR sequences is around 10^{13}, which means that T cells can recognise a huge diversity of antigens, including self-antigens [29, 33, 34]. Despite the huge diversity of TCR sequences, we observed that the frequency was not similar among TCR clonotypes. Moreover, in a cancer context, the response to immune checkpoint inhibitors may be correlated to broad diversity and frequency of TCR clonotypes [35].

Table 1. Number of segments in each region of TCR-β in mouse [36].

TCRβ	Functional gene
TRBV	22
TRBD	2
TRBJ	11
TRBC	2

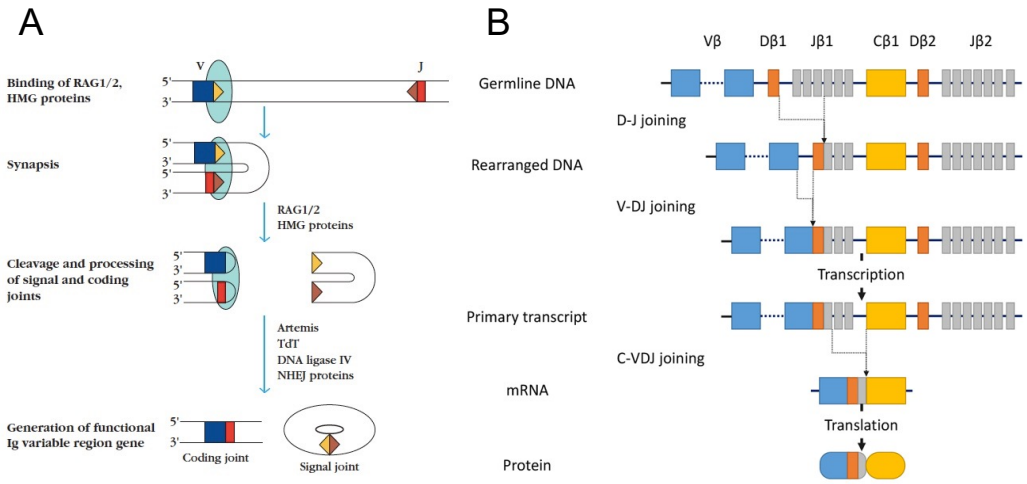

Figure 2. Schematic representation of TCRβ rearrangement. (A) The Rag1/2 enzymes recognize and cleave in a specific sequence at the end of the segment of the V region and an initial sequence of the segment of the J region. After that, the TdT enzyme add some nucleotides and a complex of enzymes ligate the two segments. (B) Segments of D and J regions are rearranged in first followed by V-DJ rearrangement. Subsequently, a segment of C region joins to VDJ regions, finally forming a functional TCR. Reprinted from (A) [36]; (B) [37].

When T cell precursors are capable of expressing the TCR on their cell surface, these cells acquire a double positive (DP) phenotype: $CD4^+CD8^+$ [28]. DP thymocytes are then prone to interact with antigens presented by MHC complexes from cortical thymic epithelial cells. T cell avidity will then determine the fate of thymocytes: if T cells show low avidity between their TCR and the antigen presented by major histocompatibility complex (MHC) class I or MHC class II molecules, they become $CD8^+$ or $CD4^+$ T cells, respectively. On the other hand, if T cell precursors show no avidity, they will be eliminated by neglect. This process is called positive selection and is followed by the migration of single positive (SP) thymocytes to thymus medulla. Here, SP thymocytes interact with self-peptide-MHC complexes presented by medullary thymic epithelial cells: low avidity interactions lead their exit from the thymus, while high avidity lead to elimination through negative selection [27]. However, this process is rather complex, as thymocytes that show an intermediate level of avidity to self-antigens are not eliminated by the negative selection, but give raise to Tregs, a special lineage of $CD4^+$ T cells.

Subsequently, T cells are able to differentiate into different subsets [38]. Naïve $CD8^+$ T cells differentiate into cytotoxic T cells whereas naïve $CD4^+$ T cells can differentiate into two groups of cells: $CD4^+$ effector T cells ($CD4^+$ T_{eff} cells), such as T helper (Th)1 and Th17, among others and Tregs. This process of differentiation occurs by the action of specific cytokines, such as Il-2, Il-6 and TGF-β (Figure 3) [38, 39].

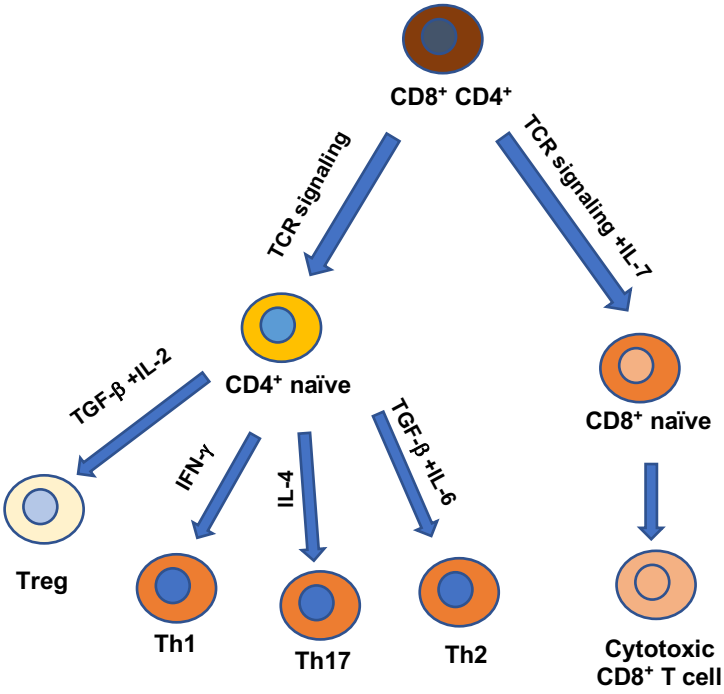

Figure 3. Schematic representation of the T cell differentiation from double positive cells and the main extracellular signals that induce this differentiation. Adapted from [39].

1.4. Immunotolerance

Immunotolerance is an important natural mechanism in homeostasis, as it allows the immune system to tolerate self-peptides and some environment peptides, preventing reactivity against self-cells and tissues. Deficiencies in this process often lead to allergies or autoimmune diseases like immune dysregulation, polyendocrinopathy, enteropathy, X-linked (IPEX) syndrome, type 1 diabetes, autoimmune polyendocrinopathy-candidiasis-ectodermal dystrophy (APECED), among others [40, 41].

It can be divided in two different parts, depending on the site where T cell tolerance is induced: central tolerance, if arising at the site of lymphocyte development, the thymus; or peripheral tolerance, if arising in peripheric tissues [40].

This mechanism is also exploited by tumour cells to escape from the immune response and, thus, promote invasion and/or metastasis formation [42]. The major contribution for that to happen relies on the fact that malignant cells arise from the own host cells and therefore, most tumour cells express self-antigens to which T cells have been tolerized [43].

As a result, some immunotherapy approaches have focused on disrupting cancer immunotolerance by the adoptive transfer of immune effectors, the use of immunomodulatory therapy and vaccination [44] . Recently, chimeric antigen receptor (CAR) T cells, which are genetically modified to be reactive against tumour antigens, have been used in small clinical trials and FDA has already approved two CAR-T therapies [45].

This shows that immunotolerance is a field with a lot of potential that may result in the appearance of novel approaches to treat cancer patients [44].

1.4.1. Central tolerance

Central tolerance is acquired in the thymus by deletion of autoreactive T cells or by the development of Tregs [46]. The former process is collectively known as clonal deletion because it eliminates most of autoreactive T cells. It represents one of the main strategies to guarantee central tolerance [46]. The latter mechanism is known as clonal diversity, where a special subset of $CD4^+$ T cells, known as Tregs, is formed. These cells recognise self-antigens with intermediate affinity and, thus, are not deleted by negative selection [47]. Therefore, they suppress possible immune responses in the periphery by certain autoreactive T cells that may go through negative selection without elimination [46].

Besides that, some reports show that some self-antigens expressed in the thymus may be tumour antigens that, in turn, lead to the tolerization of T cells against tumour cells in the context of tumour evasion [48, 49]. Additionally, peripheral dendritic cells can transport antigens to the thymus, where they present them to T cells, reinforcing the role of central tolerance which can be used by tumour to tolerate neoantigens [50-52].

1.4.2. Peripheral tolerance

Central tolerance alone is insufficient to prevent autoimmunity or allergic diseases since not all antigens that are needed to tolerate T cells are expressed in the thymus, such as food antigens [46, 53]. Moreover, the efficacy of negative selection is not perfect and, for this reason, some autoreactive T cells may exit from the thymus [54]. Not surprisingly, an additional mechanism exists, peripheral tolerance. Through it, T cells that react against self-antigens or some environment/ non self-antigens, in the periphery, are identified and inhibited, and the tolerance to the gut microbiome and food antigens is safeguarded [46]. The mechanism of peripheral tolerance includes direct suppression of effector T cells by induction of anergy or apoptosis and conversion of T cells into Tregs [42].

There are many pathways to induce anergic T cells, one of them is by tolerogenic/immature dendritic cells, which did not reach full maturation. Therefore, antigen presentation and subsequent recognition by T cells is not sufficient to activate and induce proliferation of these cells, as these APCs do not deliver the adequate co-stimulatory signals [46]. In addition, Tregs can stimulate T cell anergy state through the expression of certain cytokines, such as Il-10 and TGF-β. Furthermore, some negative stimulatory molecules such as CTLA-4 and PD-1/PD-L1 can also lead to T cell anergy, and some reports show that animals with

loss of CTLA-4 or PD-L1/PD-1 present abnormal lymphoproliferation and autoimmunity [46, 54-57] .

Not only immune cells can induce this anergy state, but instead, in non-small cell lung cancer (NSCLC), melanoma, and other types of tumours, these immune checkpoint ligands are highly expressed, showing that tumour cells can express these negative co-stimulatory ligands in order to promote their tolerization [46, 58, 59].

In the case of induction of apoptosis of autoreactive T cells, Fas (CD95) and Bim seem to have an important role for peripheral tolerance. These are involved in death pathways and animals deficient for both proteins have been shown to lose peripheral tolerance, with an increase in the number of T cells, mainly in the lymph nodes and spleen [54, 60-62].

In the tumour site or in peripheral tissues, T effector cells can be converted to Tregs, and, despite the mechanisms being still poorly understood, the presence of TGF-β and IL-2 seems to have an impact in this conversion to a more “tolerogenic” profile [63-65].

Overall, Tregs have an important role in maintaining homeostasis at peripheral sites and this tolerance can be used by tumour cells to create an immunosuppressive microenvironment [43].

1.5. Immunotolerance induced by cancer cells: role of regulatory T cells

Regulatory T cells are one subtype of $CD4^+$ T cells originally discovered by Sakaguchi in 1995 as a $CD4^+CD25^+$ population of lymphocytes with the ability to suppress other immune cells in response to self-antigens [66]. For this reason, these cells are known to be involved in the prevention of autoimmune diseases, as well as in controlling the inflammatory response, anti-tumour immunity, among others. Nevertheless, the characterisation of this type of T cells was ambiguous because the CD25 marker is commonly expressed in all activated T cells, and thus, not all $CD25^+CD4^+$ T cells may have a suppressive function or represent Tregs [67, 68].

In the 2000s, the Forkhead box P3 (FoxP3) expression by Tregs was discovered [67]. Later reports asserted FoxP3 as an important marker for the characterisation of Treg populations and established this marker as crucial for the development and immunosuppressive functions of this unique lineage of $CD4^+$ T cells [46, 68]. Moreover, the development of two autoimmune disorders, IPEX syndrome in humans and scurfy in mice, are now associated with the presence of mutations in the *FoxP3* gene [68, 69]. These syndromes are a result of the loss of Tregs, showing the importance of this transcription factor [68]. Although recent reports have found transient FoxP3 expression in other T cells, it is more sustained in Tregs, continuing to be a key marker for these cells [70, 71]. Nowadays, the combination of $FoxP3^+$, $CD4^+$ and $CD25^+$ expression is commonly used to characterise the immunosuppressive Treg population [72].

Later, other markers were found such as PD-1, CTLA-4, the glucocorticoid-induced TNFR-related protein (GITR), lymphocyte activation genes (LAG-3) or inducible T cell costimulator (ICOS), but none of them were found to be exclusive for Tregs [73].

Depending on the local of origin of Tregs, these can be divided into two different groups: thymus-derived Tregs (tTregs) or peripheral Tregs (pTregs) [74]. The former, also known as natural Tregs, comprise about 6-10 % of total $CD4^+$ T cells in the peripheral blood and are formed in the thymus, as a result of intermediate avidity interactions between developing thymocytes and self-antigens-MHC complexes provided by APCs or thymic cells [46, 51, 75, 76]. This mechanism is not yet understood but, so far, it is recognized that TCR signalling strength, the presence of IL-2 and TGF-β, and *FoxP3* expression are crucial for this process [71]. Moreover, Watanabe *et al.* showed that the location within the thymus where the antigen is encountered could also be decisive for tTreg development [77].

In extra thymic tissues, pTregs are formed by conversion of $CD4^+$ T cells upon non self-antigen presentation to naïve or effector $CD4^+$ T cells and they are important in peripheral tolerance [64, 68]. To date, little is known about this process but TGF-β is thought to be involved in upregulation of FoxP3 expression, leading to the conversion of $CD4^+$ T cells into pTregs [71, 78]. Additionally, pTregs can be divided in type 1 regulatory T cells, which are important in local immunosuppression and organ transplantation [79] and T helper 3 (Th3), which are important in oral tolerance [80].

Despite the existence of different markers to characterise Tregs, it is still impossible to distinguish between pTreg and tTreg populations, due to unspecificity for Treg lineage and to transient expression profiles in certain cases. Therefore, a lot of work has been done to define new specific markers, especially at the membrane, that can distinguish these populations in order to evaluate if they present distinct functions and/or antigen specificities [81-83]. Furthermore, this knowledge will be crucial for the understanding of the mechanism of each subset in the context of cancer or autoimmune diseases, and, consequently, for the development of putative immunotherapeutic strategies to target these cells [81].

Recently, two markers have been considered to distinguish these two populations: Helios and Neuropilin-1 (NRP1). Thornton *et al.* described the expression of Helios, a member of the Ikaros transcription factor family, as being important in lymphocyte development and as specific marker to distinguish pTregs from tTregs, in both humans and mice [82]. According to this author, all $CD4^+CD8^-FoxP3^+$ thymocytes express Helios and 70% of Tregs in peripheral lymphoid tissue are $Helios^+$, therefore being tTregs [82]. Still, several other reports demonstrated that Helios was not an efficient marker to distinguish the tTreg and pTreg, since it was expressed in the presence of antigens, showing to be a better marker for activation than characterisation of the Treg lineage [84, 85]. Additionally, Szurek *et al.* compared $Helios^{high}$ and $Helios^{low}$ cells against their TCR repertoire and the comparison

obtained indicated no differences between these populations [81]. Later, Yadav and his colleagues identified NRP1 protein as a new marker of tTregs [83]. In an experiment conducted using induced Tregs, they showed that these cells express low or undetectable NRP1 levels and, as a consequence, a high expression of this marker would be synonymous to tTregs [83]. However, Szurek *et al.* published contradictory results showing that NRP1 was not a good marker for tTregs since the TCR repertoire between $NRP1^{low}$ or $NRP1^{high}$ cells was very similar, meaning that both lineages were comparable [81]. For this reason, the use of both markers to distinguish these subsets should be used with caution, and other markers are still required for a complete separation of Tregs regarding their origin [81].

Despite the lack of markers to distinguish between pTregs and tTregs, and thus, the inability to explore Treg origin, the presence of Tregs in tumour site is of major importance, as shown by solid evidence from multiple reports [86, 87]. Nevertheless, the existence of tumour-infiltrating Tregs (tiTregs) has different prognostic values, depending on the type of cancer [86]. In studies with patients with head and neck squamous cell carcinoma [73], breast cancer [88], melanoma [89] or pancreatic ductal adenocarcinoma [90], for example, the presence of tiTregs is associated with poor prognosis. In contrast, patients with colorectal adenocarcinoma [91] or follicular lymphoma [92], the presence of tiTregs is associated with a good prognosis. Interestingly, an explanation has emerged for some of these controversial results. In the case of colorectal cancer, which has a good prognosis in the presence of tiTregs, the inflammation provoked by certain bacteria which promotes carcinogenesis is suppressed by Tregs and, thus, can benefit the host [73].

The recruitment of Tregs and expansion at the tumour site can occur by different mechanisms. One of them is chemoattraction promoted by chemokines released by cancer or innate immune cells. Some pairs of C-C motif chemokine ligand (CCL) and C-C chemokine receptors (CCR), such as CCL17/CCL22-CCR4, CCL5-CCR5 or CCL20-CCR6 and CCL28-CCR10, are involved in this recruitment [74, 93, 94]. In addition, accumulation of Tregs in cancer may be explained by the release of molecules, such as TGF-β, which promote the differentiation from effector T cells to Tregs and their proliferation [74, 95]. The suppressive capacity of tiTregs is higher at the tumour site than in peripheral blood, and it may derive from activation of Tregs after exposure to tumour antigens. Because tumour antigens derive from self-antigens, Tregs are preferentially activated compared to effector T cells [74, 96].

Once activated, Tregs can supress a high range of immune cells and there are several pathways through which Tregs can do this, namely by the release of soluble factors like TGF-β, IL-10, perforins and granzymes (Figure 4) [87, 97]. In addition, expression of immune checkpoint molecules such as CTLA-4, LAG-3 and ICOS is associated with

enhanced suppressive activity and promotion of tumour progression [22, 74, 97]. The consumption of IL-2 and the expression of CD39 and CD73, which can convert exogenous ATP into adenosine, act synergically to inhibit effector T cells [22, 97]. A recent study by Akkaya *et al.* has reported that antigen specific Tregs have the ability to remove the specific MHC-peptide complex from dendritic cells, demonstrating a new mechanism for T cell suppression that may also justify why some immunotherapeutic strategies do not work [98].

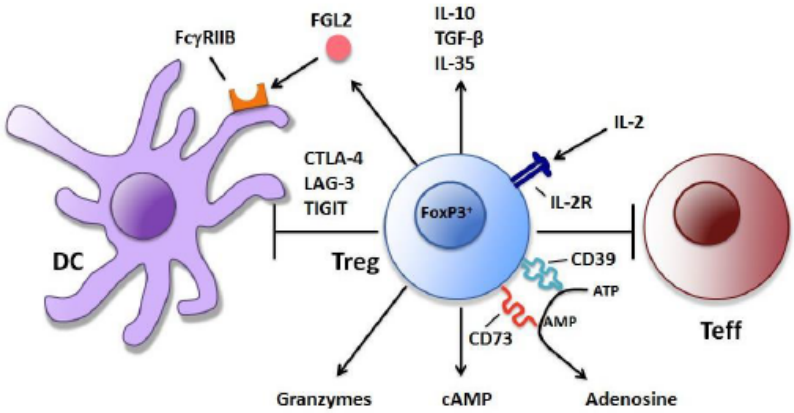

Figure 4. Suppression mechanisms used by Tregs to inhibit APC and effector T cells. Reprinted from [99].

In summary, there is a lot of evidence supporting the importance of tolerance in tumour escape from the immune response. More specifically, Tregs have been identified as the main players in this context. A lot of work has been done to better understand the activity and recruitment of these cells but there is still a lot that remains to be elucidated. More importantly, it is necessary to understand the origin of tiTregs and their function regarding their lineage. Thus, the identification of good markers to distinguish these populations will be key for the development of new treatments against cancer in the future.

2. Aim

It is clear that immunotolerance has a big impact in tumour progression. Tregs may be the main factor contributing to immune suppression in cancer, and their presence is associated, in some cases, with a worse prognosis. For this reason, it is important to better dissect the role of tiTregs, namely their origin, function, markers and recruitment to the tumour site.

Despite the fact that some suppressive mechanisms were already identified, Treg lineages and their impact in tumour development are poorly understood.

To clarify that, the main goal of this work is to determine the origin of tiTregs. We hypothesized that the Treg population in the tumour site may be both pTregs and tTregs showing the importance of both types of tolerance, peripheral and central, in tumour immune escape.

Specific objectives for this work included:

1- Assessing the presence of Tregs in the tumour site of two different mouse models: an inducible mouse model of colorectal cancer, the $Lrig1^{CreERT2/+}$;$Apc^{flox/+}$ mice and MC38-derived subcutaneous tumours in $FoxP3^{eGFP.DTR.Luci}$ mice. The analysis and characterisation of the tumours infiltrate were performed by flow cytometry and immunohistochemistry.

2- Determining the origin of tiTregs by comparing the TCR-β sequences between tumour-infiltrating Tregs and $CD4^+$ T_{eff} cells, using next-generation sequencing (NGS). If the TCR-β sequences show a match between both cell types, it indicates peripheral conversion, whereas if they are different, it directs to a central origin of Tregs.

3. Material and Methods

3.1. Cell line

The C57BL/6 mouse-derived colorectal adenocarcinoma cell line MC38 was purchased from Kerafast (Boston, MA, USA). Cells were grown in recommended complete medium: RPMI 1640 with L-Glutamine medium supplemented with 10% heat inactivated Fetal Bovine Serum (FBS) (both from Biowest, Nuaillé, France) and 1% Penicillin-Streptomycin (GIBCO®, Life Technologies, Carlsbad, CA, USA), and kept under conventional cell culture conditions, in a humidified atmosphere containing 5% of CO_2 at 37ºC.

When cultures reached approximately 80% of confluence, subculture was performed. For this purpose, the medium was removed from the flask and cells were washed with Trypsin-EDTA solution (0.05% trypsin, 0.02% EDTA) (Sigma-Aldrich®, St. Louis, MO, USA) and left in the incubator until cells were detached from the flask surface. Trypsin activity was then blocked with FBS, present in the complete RPMI medium that was added to the cell suspension at this point. Cells were transferred to a Falcon tube and centrifuged at 1200 rotations per minute (rpm) for 5 minutes (min) ((Centrifuge 5810, rotator A-4-62, (Eppendorf, Germany)). After discarding the supernatant, the cell pellet was resuspended in complete medium and seeded in new flasks/tubes.

The cell line used in this work was tested for Mycoplasma spp. This possible contamination was assessed by PCR using specific primers for 16S RNA of Mollicutes (forward primer, GPO1: 5'- ACT CCT ACG GGA GGC AGC AGT A – 3' and reverse primer, MGSO: 5'- TGC ACC ATG TGT CAC TCT GTT AAC CTC – 3' [IDT – Integrated DNA Technologies, Coralville, IA, USA]).

3.2. Mice

In this dissertation, two different mouse models were used: $Lrig1^{CreERT2/+}$;$Apc^{flox/+}$ mice and $FoxP3^{eGFP.DTR.Luci}$ mice, kindly gifted by Prof. Robert J. Coffey (Vanderbilt University Medical Center, USA) and by Prof. Natalio Garbi (University of Bonn, Germany), respectively.

All mice were housed in a specific pathogen-free environment under strictly controlled light cycle conditions (12 hours of light/dark), and allowed a standard rodent chow, and water *ad libitum.*

All experiments using animals were carried out with the permission of the local animal ethical committee in accordance with the European Union Directive (2010/63/EU) and Portuguese law (DL 113/2013). The experimental protocol was approved by the ethics committee of the Portuguese official authority on animal welfare and experimentation (Direção-Geral de Alimentação e Veterinária – DGAV).

3.2.1. Lrig1$^{CreERT2/+}$;Apc$^{flox/+}$ mice

The Lrig1$^{CreERT2/+}$;Apc$^{flox/+}$ mouse model, described by Powel *et al*., was chosen as an inducible model and conditional genetically engineered mouse model (GEMM) of intestinal tumorigenesis [100].

These mutant mice were generated with insertion of a tamoxifen-inducible Cre recombinase (CreERT2) into the translational initiation site of the endogenous Leucine-rich repeats and immunoglobulin-like domains 1 (Lrig1) locus and the insertion of LoxP sites flanking the exon 14 of the *Apc* gene.

These animals were injected with 2 or 4 mg of Tamoxifen (Sigma-Aldrich®, St. Louis, MO, USA) diluted in corn oil (Sigma-Aldrich®, St. Louis, MO, USA) by intraperitoneal injection, once a day for 3 consecutive days, leading Lrig1^{+} progenitor cells to lose one copy of the *Apc* gene. Then, the spontaneous loss of heterozygosity of the second *Apc* allele results in a predictable pattern of neoplastic lesions, culminating in multiple, highly dysplastic tumours along the small and large intestine. For that reason, animals were monitored for weight, appearance and behaviour once a week. Additionally, after 50-70 days of tamoxifen induction, mice were monitored by colonoscopy every 20-30 days for signs of tumour formation in the distal colon.

The euthanasia procedure, done by cervical dislocation was performed when the animal reached a humane endpoint due to advanced disease (100-310 days after induction, with tumour burden varying from mouse to mouse).

In all experiments of our study, heterozygous mice for CreERT2 and Apc^{flox} were used to guarantee the expression of Lrig1 and that the second hit in the *Apc* allele occurs later. Lrig1-WT, Lrig1^{CreERT2} and Apc^{flox} allele were identified by PCR from genomic DNA of ear punch biopsies using the following primers: for Lrig1- WT (forward primer - TCTGGCTGCTCTTGCTGCTACT, reverse primer - GACTTCACGAGGCACACTCGAT) for Lrig1^{CreERT2} (forward primer - TCATCGCATTCCTTGCAAAAGT reverse primer - GACTTCACGAGGCACACTCGAT and for *Apc* allele (forward primer-5′- GGCTCAGCGTTTTCCTAATG) reverse primer- 5′- GATGGGTCTGTAGTCTGGG) (IDT – Integrated DNA Technologies, Coralville, IA, USA).

3.2.2. FoxP3$^{eGFP.DTR.Luci}$ mice

The FoxP3$^{eGFP.DTR.Luci}$ mice are bacterial artificial chromosome (BAC) transgenic mice, generated by Suffner *et al*. [101]. In this transgenic mouse model, a construct composed of the cDNAs for enhanced green fluorescent protein (eGFP), human diphtheria toxin receptor (DTR) and luciferase gene was inserted at the start codon (ATG) in the third exon of the *FoxP3* gene and randomly integrated into the genome of the C57BL/6 (B6) mouse. The

coding sequences were separated by a self-cleaving 2A peptide sequence for stoichiometric production of the three individual transgenic proteins.

All experiments were performed using heterozygous animals for the transgenic construct.

Typing was carried out by PCR from genomic DNA of ear punches biopsies using the following primers: DTR Forward – 5´GCCACCATGAAGCTGCTGCCG3' and DTR Reverse – 5' TCAGTGGGAATTAGTCATGCC3' (IDT – Integrated DNA Technologies, Coralville, IA, USA).

3.3. Animals procedures

3.3.1. Subcutaneous tumour induction

In the case of FoxP3$^{eGFP.DTR.Luci}$ mice, the MC38 tumour cell line was injected subcutaneously to induce tumour formation.

On the injection day, cultured cells were collected from the tissue culture flask, centrifuged and resuspended in PBS (Fisher Scientific, Hampton, New Hampshire, EUA). Cellular viability was measured, in order to inject healthy cells in the animals, through dilution with Trypan Blue dye (Gibco®, ThermoFisher Scientific, Waltham, MA, USA). Viable cells were automatically counted by an TC20^{TM} automatic cell counter (Bio-Rad, Hercules, CA, USA). The animals were anesthetised by isoflurane inhalation, and 1x10^6 MC38 cells were injected subcutaneously in 100 µl of saline solution.

They were monitored every 2/3 days after the injection in terms of behaviour, weight, appearance and tumour size. A digital caliper (Toolland, Gavere, Belgium) was used to measure two perpendicular dimensions of the tumour: the longitudinal diameter (length) and the transverse diameter (width). Tumour volume was estimated by the modified ellipsoidal formula $V = \frac{LW^2}{2}$, where L is the length and W is the width.

Mice were euthanized by cervical dislocation between 20-30 days after MC38 inoculation or when tumour size reached 2000 mm^3, the animal became moribund or tumour ulceration was appeared.

3.3.2. Colonoscopy

Colonoscopy was used to monitor tumour development in the Lrig1$^{CreERT2/+}$;Apc$^{flox/+}$ mice (Figure 5).

The Mainz Coloview mini-endoscopic system [KARL STORZ, Tuttlingen, Germany] was used to perform colonoscopies on the mice. The animals were anesthetised before they received an enema with 100-150 µl of saline solution (0.9% NaCl) using a catheter. After the mouse expelled the faeces, colonoscopy was started inserting the endoscope with a

camera in the anus, applying air flow to inflate the colon and the appropriate lighting for proper visualization.

After some images of the colon were captured the endoscope was removed, and the animal placed in its respective cage and monitored until regain of consciousness.

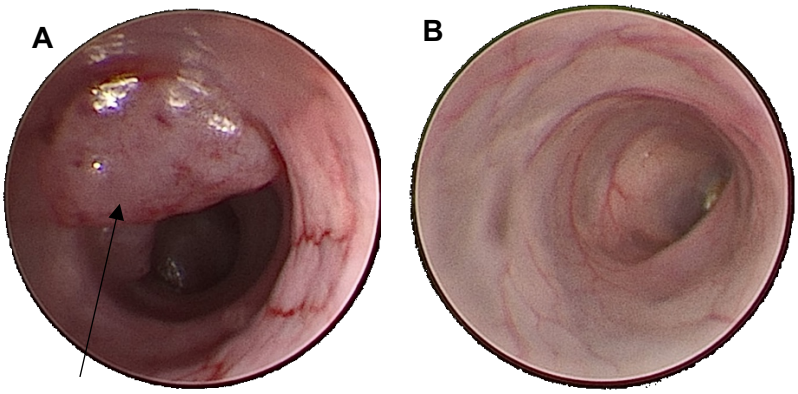

Figure 5. Representative colonoscopy images from tumour development in Lrig1$^{CreERT2/+}$;Apc$^{flox/+}$ mice performed between 50 days after the injection of tamoxifen and on the day of the euthanasia. (A) a visible tumour showing an advanced stage of tumour development; (B) no macroscopic visualization of tumours.

3.3.3. Blood collection

To collected blood samples, cardiac puncture was performed before cervical dislocation. As this is an invasive approach, it was performed in an anaesthetic state using isoflurane inhalation. Briefly, a syringe with a 25 G needle was inserted on the animal´s side, bellow of the elbow until it reached the animal's heart. The blood collected was inserted in a K3 EDTA tube (AQUISEL®, Barcelona, Spain), which has an anticoagulant substance.

3.4. Collection of single-cell suspension from different tissues

3.4.1. Tumour

Tumours collected from Lrig1$^{CreERT2/+}$;Apc$^{flox/+}$ mice were cut into 2-3 µm pieces and were then incubated with collagenase IV solution (90% RPMI 1640 with L-Glutamine medium, 10% FBS, 1 mM $CaCl_2$, 1 mM $MgCl_2$ and 100 U/ml collagenase IV) in a thermoblock (VWR^{TM}, Radnor, PA, USA) at 37 ºC and 600 rpm for 30 min. The volume of tumour should be less than 1/3 of volume of collagenase IV solution to facilitate the digestion. Subsequently, the sample was passed through a 70 µm cell strainer (Corning®, Sigma-Aldrich®, St. Louis, MO, USA) and was washed until a single-cell suspension was obtained. Afterwards, a centrifugation step of 5 min at 1700 rpm was performed and the pellet was resuspended in 1 ml of FACS Buffer (PBS (1X) + 2% FBS). Cellular viability was assessed by the same approach as previously described (Section 3.3.1.).

The digestion of MC38-derived subcutaneous tumours was very similar to the approach performed for Lrig1$^{CreERT2/+}$;Apc$^{flox/+}$ tumours. Despite the samples being larger than the intestinal tumours, they went through two additional phases, one before the incubation of the thermoblock and another after this, using the gentleMACS™ Dissociators (MACS, Miltenyi Biotec, Germany) to facilitate the tissue digestion. Moreover, after determining the cellular viability, the samples were enriched to hematopoietic cells, by performing the positive selection of CD45$^+$ cells using magnetic activated cell sorting CD45 Microbeads (MACS, Miltenyi Biotec, Germany) and LS separation columns according to the manufacturer´s instructions. Briefly, cells were labelled with CD45 Microbeads and the cells suspension passed through a LS column, which is placed in magnetic field of MACS separator, being the CD45$^+$ T cells retained in the column. Later, the column was removed from the magnetic field and CD45$^+$ T cells were eluted. Finally, the cellular viability was determined (Section 3.3.1).

3.4.2. Spleen

In order to obtain single-cell suspensions from spleens, manual disruption was performed to digest the organ using a syringe plunger against the tissue in a 70 µm cell strainer (Falcon®, Corning, Tewsbury, MA, USA). The sample was centrifugated at 1700 rpm for 5 min at 4 ºC (Centrifuge 5810R, S-4-104 Rotor, (Eppendorf, Germany)), the supernatant was removed and the pellet was resuspended in 5 ml Red Blood Cell Lysis Buffer (1 volume of Tris hydrochloride (Tris-HCl) + 9 volumes of ammonium chloride (NH_4Cl)) and incubated for 5 min at room temperature (RT).

Finally, the samples were re-centrifuged using the same conditions as mentioned above and resuspended in 1 ml of FACS Buffer. The number of viable cells was assessed as previously described (Section 3.3.1).

3.4.3. Blood

After blood collection, the sample was centrifuged at 1200 g for 10 min and the supernatant was discarded. Then, the pellet was resuspended in 5 ml Red Blood Cell Lysis Buffer and incubated for 5 min at RT. Later, two more centrifugations were performed for 5 min at 1700 rpm, followed by pellet resuspension in 1ml of FACS buffer, in both centrifugations. Finally, viable cells were collected and assessed as previously described (Section 3.3.1).

3.5. Immunohistochemistry and H&E staining

To prepare samples for haematoxylin and eosin (H&E) staining and immunohistochemistry analysis, tumours were collected from $Lrig1^{CreERT2/+}$;$Apc^{flox/+}$ mouse and each one was placed in a tissue processing/embedding cassette, properly identified with the identification of the animal and its localisation, and immersed in 10% formalin (Bio-optica, Milan, Italy). After 24 hours, tissue processing was performed, where cassettes and tissues were immersed in a sequencing of solutions: 70% ethanol, 80% ethanol, 90% ethanol, 2 consecutive rounds in 100% ethanol, 3 rounds in Clear Rite for 1 hour each and 2 rounds in Paraffin for 1 hour and 20 minutes each. Lastly, tissues were embedded in paraffin wax for later analysis of histological sections.

Using a microtome (Micron HM 335E), tissue sections of 4 µm were obtained and fitted in coated slides (Thermofisher Scientific, Waltham, MA, USA) and then they were incubated overnight at 37 ºC and stored at RT until perform immunohistochemistry or H&E assay.

To perform an immunohistochemistry assay, firstly the tissue was deparaffinised through immersion of the slide in xylene solution (VWR, Radnor, PA,USA) in two rounds of 5 minutes and then hydrated with 100% ethanol for 5 min and two rounds of 5 min with 70% ethanol followed by incubation for 5 min under running water.

Next, the antigen retrieval was executed by putting antigen unmasking solution retrieval with pH6 citrate-based buffer (Vector Labs, Burlingame, CA, USA) in slides and into a water vaporizer machine for approximately 35 min at 99 ºC. Afterwards, slides were left at RT to cool down and subsequently washed twice in 0.1% (v/v) PBS-Tween solution (PBS-T) (Tween 20, (Sigma-Aldrich®, St.Louis, MO, USA)) for 5 min with agitation.

Later, the slides were incubated for 15 min with 3% hydrogen peroxide (Sigma-Aldrich®, St. Louis, MO, USA) in methanol (VWR, Radnor, PA, USA) to inactivate the endogenous peroxidases and washed in two rounds of PBS-T, as previously described.

Tissue sections in slides were delimitated using a hydrophobic pen (Vector Labs, Burlingame, CA, USA) and then using the appropriate volume of Ultravision Protein block solution (Thermofisher Scientific, Waltham, MA, USA) to cover the whole tissue section, the incubation was performed for 15 min at RT. The next step was the incubation with the anti-FoxP3 antibody, ab54015, (Abcam, Cambridge, UK), previously optimized to diluted 1:1000 in ready to use Antibody diluent OP Quanto (Thermofisher Scientific, Waltham, MA, USA) in a humidified chamber for 1 hour at RT. A negative control was performed in each sample, in which, instead of adding primary antibody, PBS was utilized. After the slides were washed in PBS-T for 5 minutes, with gentle agitation to remove excess of primary antibody, they were incubated with secondary antibody diluted 1:100 Swine Anti-Rabbit Immunoglobulins/Biotin (Agilent, Santa Clara, CA, USA) for 30 min at RT.

A washing step with PBS-T was performed again as mentioned above and followed by incubation with streptavidin (Lab Vision™ Ready-To-Use Streptavidin Peroxidase, (Thermofisher Scientific, Waltham, MA, USA)) for 30 min at RT.

The interaction of biotin and streptavidin was detected through the use of Dako REAL™ Diaminobenzidine (DAB) diluted 1:20 in substrate buffer in which a brown staining was produced at the site of reaction. The interaction with DAB was stopped by washing slides under running water for 5 min when the brown colour became visible on the slide or a maximum of a minute. Subsequent slides were incubated in haematoxylin solution (MercK, Darmstadt, Germany) for one minute to stain the nucleus and, then, a wash under running water was done for 5 min. Slides were dehydrated with ethanol (70% of ethanol solution for 5 min and two rounds in 100% ethanol for the same time) followed by two rounds of incubation of 5 min with xylene solution. Ultimately, DPX mounting medium (Sigma-Aldrich®, St.Louis, MO, USA) was used to mount coverslip (Normax, Marinha Grande, Portugal) on slides.

To analyse the tumour histology, H&E staining was performed. The slides were incubated twice in 100% xylene solution for 5 min followed by two rounds of immersion in 100% ethanol for 5 min and one cycle of incubation of 70% ethanol was performed. Subsequently, the slides were washed under running water for 5 min. After the slides were stained in haematoxylin solution to stain the nucleus for 3 min, another step of incubation under running wash was performed for 12 min. Thereafter, the slides were rinsed in 70% ethanol for 20 seconds and incubated for 1 min in eosin solution to stain the cytoplasm. Afterwards, the slides were dehydrated in 70% ethanol for 5 min and 2 rounds of 100% ethanol for 5 min. An incubation of 5 min in xylene solution was performed twice and, finally, the coverslips were mounted on the slides by using DPX mounting medium.

Finally, the slides from immunohistochemistry staining and H&E staining were analysed in optical microscope.

3.6. Immunophenotyping of T cells

The immunophenotyping protocol was performed using cell suspensions from tumours, spleen and/or blood. Initially, cells from the spleen, blood and Lrig1$^{CreERT2/+}$;Apc$^{flox/+}$ tumours were blocked with Fc block in 10 µg/ml for 5 min at 4 ºC, to decrease non-specific interactions with the antibodies of interest. Afterwards, cells were stained with an antibody mix composed of anti-CD3 (FITC), 1.67 µg/mL, monoclonal; anti-CD4 (PerCP), 0.4 µg/mL, monoclonal; anti-CD25 (PE-Cy7), 2 µg/mL, monoclonal – all from eBioscience™ Thermofisher Scientific, Waltham, MA, USA – for 30 min at 4 ºC. The mix also contained a fixable live/dead dye, the Zombie NIR™ dye (BioLegend®, San diego,CA, USA).

After incubation with these antibodies, cells were fixed and permeabilized with FoxP3/Transcription Factor Staining Buffer Set (eBioscience™ Thermofisher Scientific, Waltham, MA, USA) before incubation with anti-FoxP3 (APC), 10 µg/ml, monoclonal (eBioscience™ Thermofisher Scientific, Waltham, MA, USA) for 30 min at 4 ºC. After this last incubation, cells were transferred to round bottom 5 ml tubes with filter caps (35 µm) (FALCON®, Corning Science, Tamaulipas, México) and analysed in BD FACS CANTO™ II cytometer (BD Biosciences, San Jose, CA, USA) or sorted in the BD FACS Aria™ II cytometer (BD Biosciences, San Jose, CA, USA).

MC38-derived subcutaneous tumours were also blocked with Fc block, using the same conditions as referred above. Afterwards, cells were stained with a mix composed of anti-CD4, anti-CD25 and the Zombie NIR™ dye in the same conditions as previously mentioned. Finally, cells were transferred to round bottom 5 ml tubes with filter caps (35 µm).

Figure 6A presents the gating strategy used to sort the cells of interest in blood, spleen and Lrig1$^{CreERT2/+}$;Apc$^{flox/+}$ tumours. Briefly, among single cells, viable CD4^{+}T cells were selected based on the lack of staining with Zombie NIR™ and the detection of CD3 and CD4 labelling. Among these, Tregs were defined as CD25^{+} FoxP3^{+} cells whereas CD4^{+} T_{eff} cells were considered to be FoxP3^{-} cells. The strategy to isolate Tregs and CD4^{+} T_{eff} cells from MC38-derived subcutaneous tumours was very similar, with exception of CD3 labelling (Figure 6B).

After sorting, cells were collected in lysis buffer solution (MagMAX™ mirVana™ Total RNA Isolation Kit, Thermofisher Scientific, Waltham, MA, USA).

All the data was analysed using FlowJo (V10) software (FlowJo® LLC, Ashland, OR, USA).

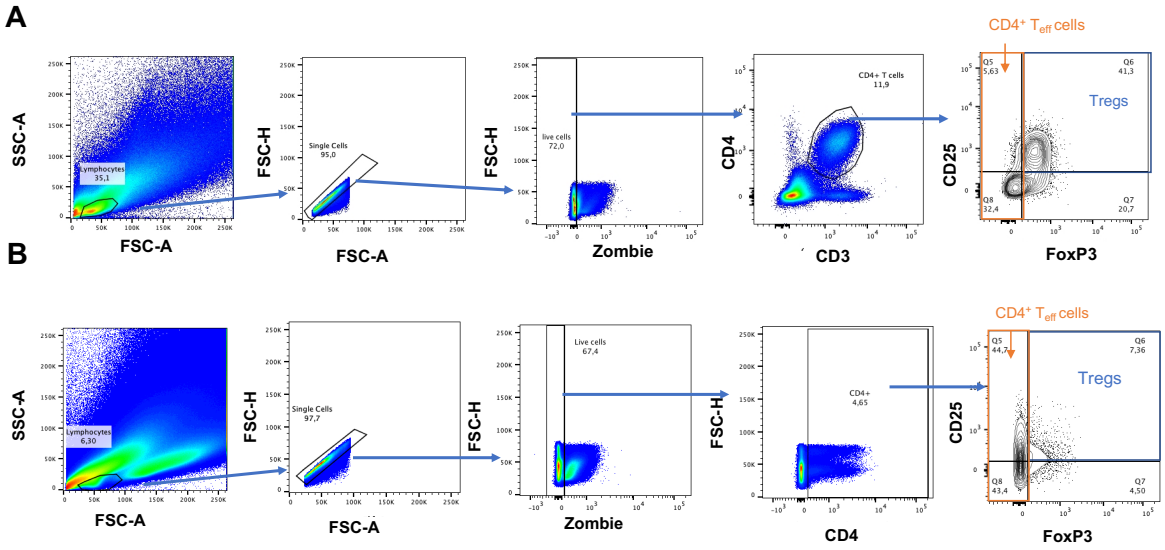

Figure 6. Gating strategy used for flow cytometry to sort populations of interest (CD4^{+}T_{eff} cells and Tregs); (A) from Lrig1$^{CreERT2/+}$;Apc$^{flox/+}$ blood and tumour samples and (B) from MC38-derived subcutaneous tumour.

3.7. RNA extraction

For RNA extraction from sorted cells, the MagMAX™ mirVana™ Total RNA Isolation Kit (Thermofisher Scientific, Waltham, MA, USA) was used. From the original protocol, two steps were adapted. First, as we collected sorted cells in the lysis buffer instead of directly resuspending a cell pellet in this buffer, the lysis buffer was diluted with FACS buffer. Second, the magnetic beads were dried at RT with the Eppendorf tube open during 4-6 min, as an alternative to shaking the beads for 2 min.

3.8. RNA quantification

After extraction, RNA was quantified using the Bioanalyzer equipment (Agilent Technologies, Santa Clara, CA, USA) to evaluate the quantity and quality of RNA. The former was obtained by RIN (RNA integrity number) that range from 1 (very fragmented) to 10 (undamaged RNA).

3.9. Sequencing of TCRβ

The RNA from sorted $CD4^+$ T_{eff} cell and Tregs was used to sequence the samples. The Ion AmpliSeq Mouse TCR Beta SR-RNA protocol (Thermofisher Scientific, Waltham, MA, USA) was followed, as instructed by the manufacturer. Briefly, a first step using the transcriptase reverse was performed, followed by amplification of the target sequences. Next, the amplicons were partially digested and the barcode plus the adapter were ligated to the amplicons. Subsequently, a quantification of the library was performed by quantitative PCR (qPCR), using the Ion Library TaqMan® Quantitation Kit (Thermofisher Scientific, Waltham, MA, USA). Finally, the template was prepared by Ion Chef and was later sequenced by Ion S5™ XL Sequencer. The data was analysed with the Ion Reporter™ software. Figure 7 is a representative TCRβ repertoire from peripheral blood (positive control).

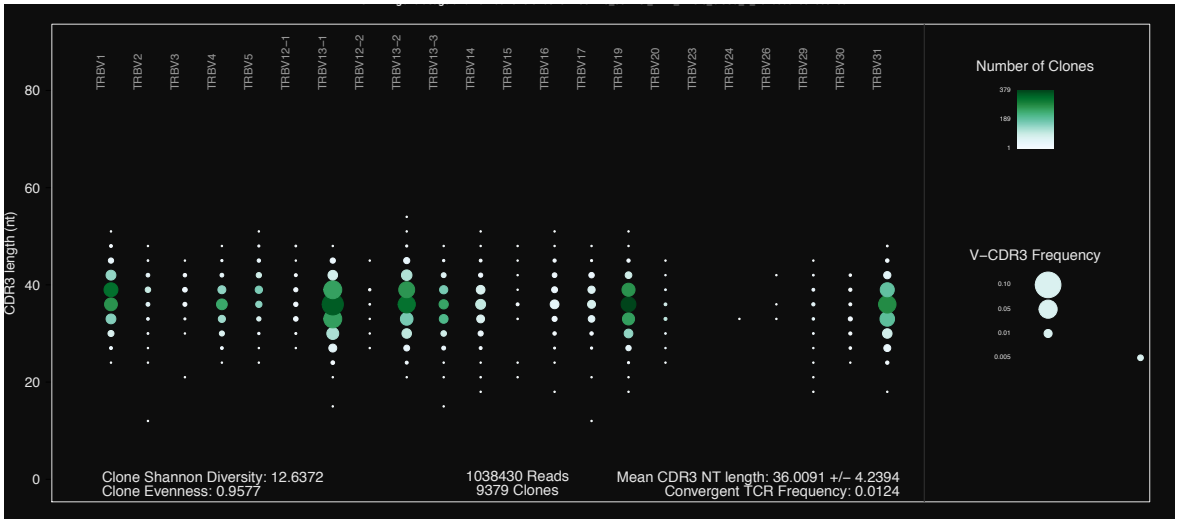

Figure 7. Representative image of TCRβ repertoire from peripheral blood sample without sorting.

3.10. Statistical analysis

Statistical analysis of the results was performed using GraphPad Prism Software (version 8).

The Kruskal-Wallis test with Dunn´s multiple comparison was used to analyse the differences in numbers and area of lesion in each part of the intestine tissue to characterise the $Lrig^{CreERT2/+}$;$Apc^{flox/+}$ mice and to evaluate the lymphocyte composition in $Lrig1^{CreERT2/+}$;$Apc^{flox/+}$ tumour applying a 95% confidence interval , with p values under 0.05 were considered significant.

To test differences between total productive reads between Tregs and $CD4^+$ T_{eff} cells from $Lrig1^{CreERT2/+}$;$Apc^{flox/+}$ blood and tumour samples, we used two-tailed Mann-Whitney test applying a 95% confidence interval and p value under 0.05 were considered significant.

In subcutaneous tumours, we evaluate also the differences in term of percentages between $CD25^-$ $FoxP3^+$ T cells and Tregs using also two-tailed Mann-Whitney test. A 95% confidence interval was applied and p value under 0.05 were considered significant.

4. Results

4.1. Lrig1$^{CreERT2/+}$;Apc$^{flox/+}$ mouse model

4.1.1. Characterisation of tumour formation

The Lrig1$^{CreERT2/+}$;Apc$^{flox/+}$ mouse model used in this study was chosen for its ability to lose one copy of *Apc* in Lrig1^{+} progenitor cells after being injected with tamoxifen. As a result, these mice develop multiple tumours in intestinal and colonic tissues after the second hit in the *Apc* gene occurs spontaneously. The animals developed tumours along the gastrointestinal (GI) tract (proximal, intermediate and distal section of the small intestine, and the cecum plus colon).

The average number and area of the lesions in each segment of the GI tract is showed in Figures 8A and B, respectively. As can be observed, most tumours sprout in the proximal area of the small intestine ($p<0.0001$, when compared to the other segments of the GI tract), with an average value of 4.77 tumours per animal. Moreover, tumour development was almost fully penetrant in this intestinal area, with only 5 out of 31 mice that did not develop any macroscopic lesions until euthanasia day. Seven mice developed tumours in the intermediate region of the small intestine, showing an average of 0.38 tumours per mouse in this area. In the distal area of the small intestine, tumour formation was observed in 6 animals, with an average number of 0.9 tumours per animal. Only 12 of 31 animals presented lesions in the colon or cecum, resulting in an average of 0.48 tumours per animal. Despite the highest number of tumours being observed in the proximal region, the largest lesions (average area in mm^2) were detected in the colon, although not statistically significant compared with other segments of GI (Figure 8B). Among 10 animals, the size (area) of tumours from the proximal segment of the small intestinal was statistical significantly higher than the lesions found in the distal part of the GI tract ($p<0.05$).

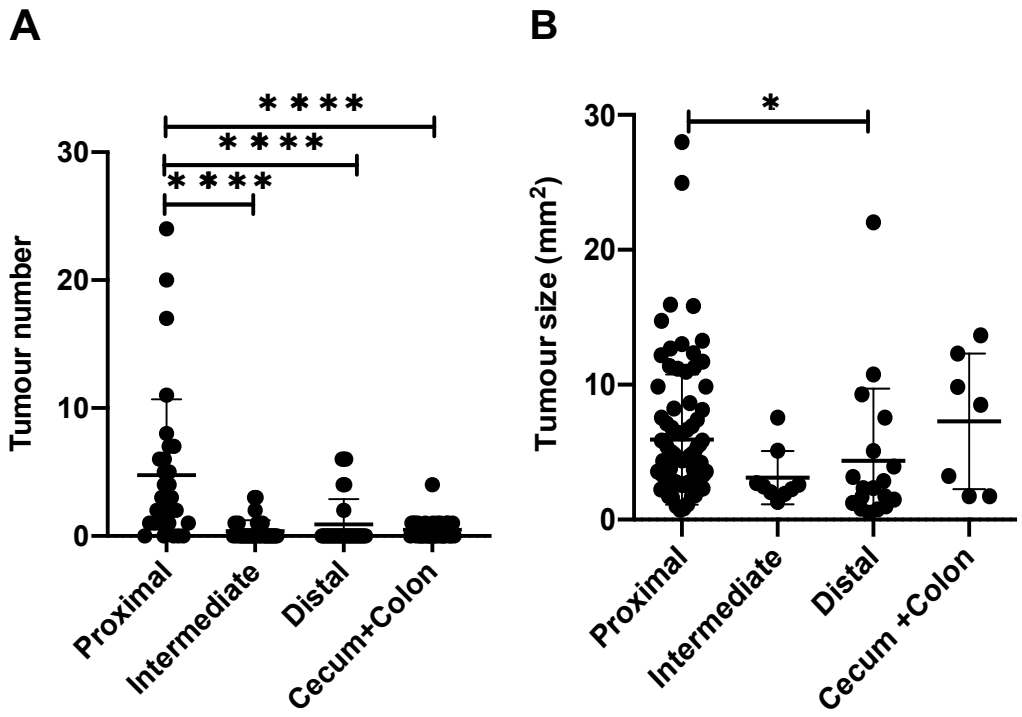

Figure 8. Distribution of tumours along the gastrointestinal tract (proximal, intermediate and distal part of the small intestinal and cecum plus colon) in Lrig1$^{CreERT2/+}$;Apc$^{flox/+}$ mice. (A) number of tumours detected in each segment of the GI tract. Each dot represents a different animal (n=31); (B) area of each lesion, in mm^2, per region of the intestine/colon, in a total of 10 mice. Each dot represents a lesion. Kruskal-Wallis test with Dunn´s multiple comparison was performed for statistical comparisons between groups. All possible comparisons between each part of GI was performed in terms of tumour number and size. Only statistically significant differences were identified with * ($p<0.05$) or **** ($p<0.0001$). Error bar is for standard deviation.

4.1.2. Immunophenotyping of spleen and tumour samples - protocol optimisation

Cells from the spleen were used to optimise the immunophenotyping protocol for detection and isolation of tumour-infiltrating lymphocytes. This organ was chosen due to the large number of lymphocytes present and the percentage of immune subsets available are already documented. Several different conditions were tested, such as the incubation time for fixation and permeabilization of cells, concentration of antibodies, temperature for antibody incubation and number of washes.

After we were able to undoubtedly isolate each population of interest in the spleen (Figure 9A) – including the isolation of the CD4$^+$ T cells and Tregs populations – we proceed to the characterisation of these populations in the tumour samples. Figure 9B shows the gating strategy used for analysis of the different populations of cells. Although not as clear as previously observed in the case of the spleen, it was possible to distinguish the cells of interest for this project.

Curiously, in the tumour samples, a population of cells that we did not detect before became apparent – the CD4$^+$FoxP3$^+$CD25$^-$ T cell population.

The herein established protocol (see Materials and Methods section 3.6) was then followed for the sorting of $CD4^+$ T_{eff} and Tregs cells from $Lrig1^{CreERT2/+}$;$Apc^{flox/+}$ tumours in the next section.

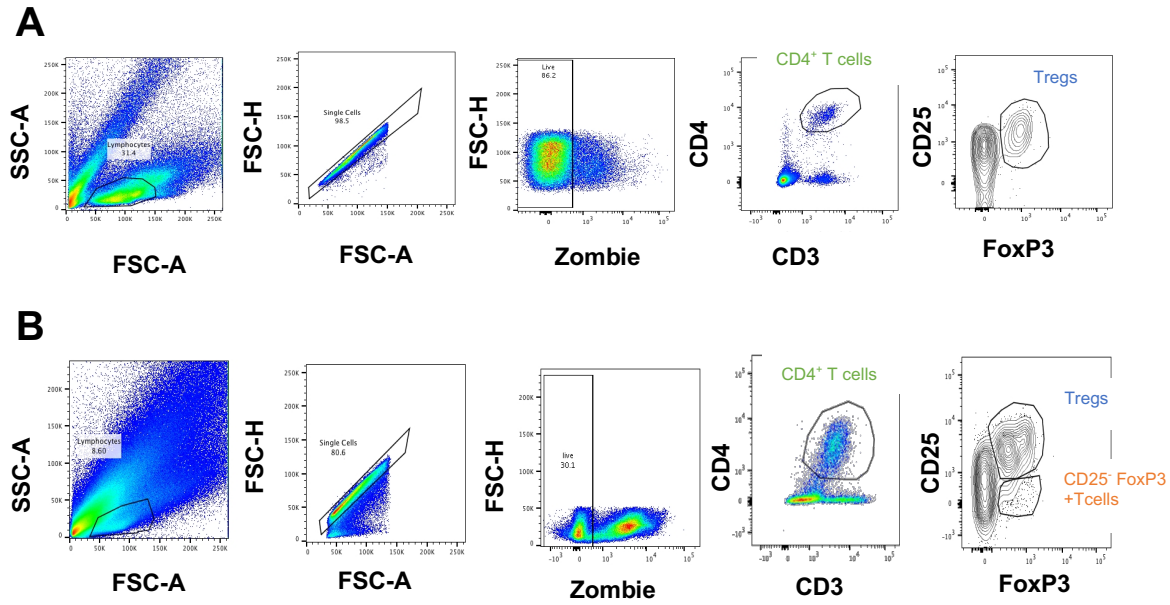

Figure 9. Gating strategy used to isolate the populations of interest after optimising the immunophenotyping protocol. (A) Flow cytometry analysis of cell suspensions from the spleen and (B) Flow cytometry analysis from $Lrig1^{CreERT2/+}$;$Apc^{flox/+}$ tumour samples.

4.1.3. Immune composition at the tumour site

After the immunophenotyping optimisation was concluded, we assessed the immune composition in tumour samples from $Lrig1^{CreERT2/+}$;$Apc^{flox/+}$ mice.

For that, we used the CD3, CD4, FoxP3, CD25 labelling and zombie (viability dye) to observe the percentage of $CD8^+$ T cells ($CD3^+CD4^-$), $CD4^+$ T cells ($CD3^+CD4^+$), Tregs ($CD3^+CD4^+$ $FoxP3^+CD25^+$) and $CD25^-FoxP3^+$ T cells ($CD3^+CD4^+CD25^-FoxP3^+$) among all viable cells (Figure 10).

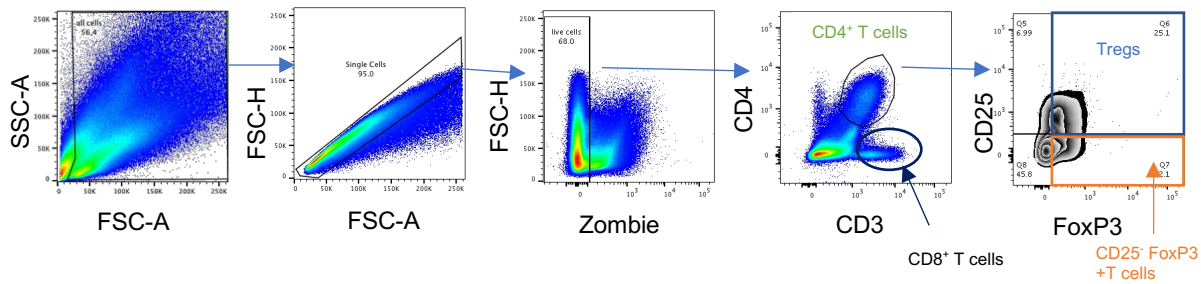

Figure 10. Analysis of tumour-infiltrating lymphocytes by flow cytometry. Among viable cells, $CD8^+$ T cells is selected by expression of CD3 and lack expression of CD4, while $CD4^+$ T cells are gated by staining of CD3 and CD4. Among $CD4^+$ T cells, the gating for Treg cells is based on the expression of FoxP3 and CD25. The gating for $CD25^-FoxP3^+$ T cells was based in the absence of expression of CD25 and strong staining of FoxP3.

Figure 11 shows the composition of immune cells from tumours samples of $Lrig^{CreERT2/+};Apc^{flox/+}$ mice. Each dot represents the analysis of tumour-infiltrating lymphocytes, in percentage of total number of cells, from a pool of tumours from one animal. As can be observed, the percentage of $CD4^+$ T cells ranged between 2.36 to 7.17% of total viable cells, with an average value of 4.73%; on the other hand, the percentage of $CD8^+$ T cells varied between 1.29 and 11.9%, with an average of 4.89%. Using a Kruskal-Wallis test, this difference in the average percentage of $CD4^+$ T *versus* $CD8^+$ T cells was not statistically significant. The average amount of Treg cells in the tumours samples was of 1%, while the percentage of $CD25^-FoxP3^+$ T cells was about 1.6%. Although being slightly higher, the percentage of $CD25^-FoxP3^+$ T cells was also not statistical significantly different from the percentage of Tregs.

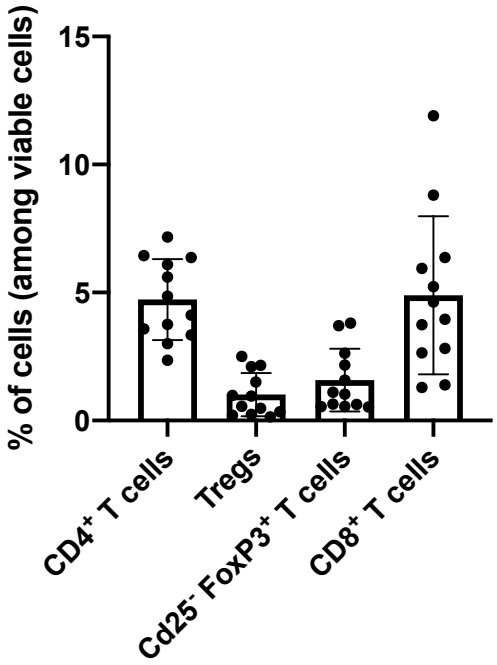

Figure 11. Immune composition of tumour samples from Lrig$^{CreERT2/+}$;Apc$^{flox/+}$ mice. Each dot represents the analysis of a pool of tumours taken from one animal. The columns show the mean +/- standard deviation of the percentage of CD4$^+$ T cells, Tregs, CD25$^-$ FoxP3$^+$ T cells and CD8$^+$ T cells in the total number of viable cells (n=12). Kruskal-Wallis test with Dunn´s multiple comparisons were performed, and no significant differences were observed between CD4$^+$ T *vs.* CD8$^+$ T cells and Tregs *vs.* CD25$^-$FoxP3$^+$ T cells pairs (p>0.05).

To confirm the presence of Treg cells and their localisation at the tumour site, histological analysis of tumours was also performed (Figures 12 and 13). Figure 12 shows the histological analysis of a colonic dysplastic lesion from Lrig1$^{CreERT2/+}$;Apc$^{flox/+}$ mouse stained with haematoxylin and eosin, where a small amount of tumour-infiltrating immune cells was observed, and most of them at the stroma site.

The presence of few FoxP3$^+$ cells intratumorally was observed by histological analysis when we performed a staining with anti-FoxP3 antibody (Figure 13). Moreover, a high density staining in normal tissue adjacent to the tumour could be observed.

In summary, the flow cytometry and histological analysis showed that Tregs were present in tumours.

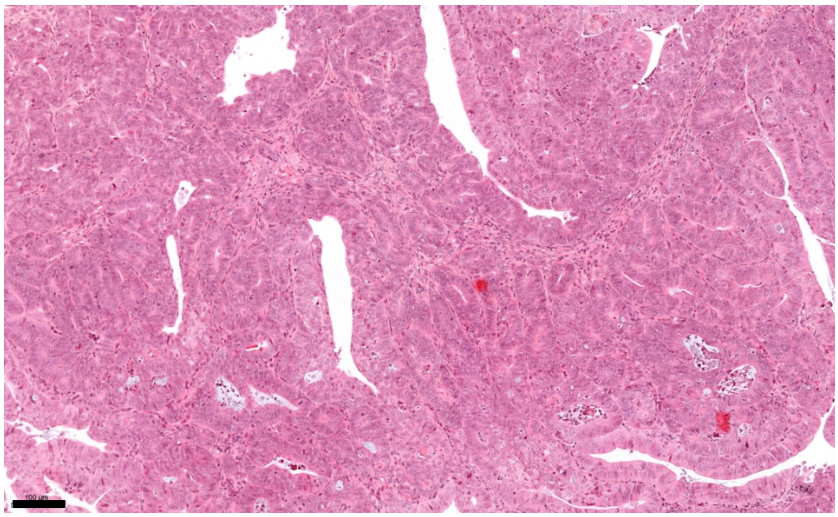

Figure 12. Representative haematoxylin and eosin staining in a colonic tumour sample from Lrig1$^{CreERT2/+}$;Apc$^{flox/+}$ mouse. Scale bar, 100 µm.

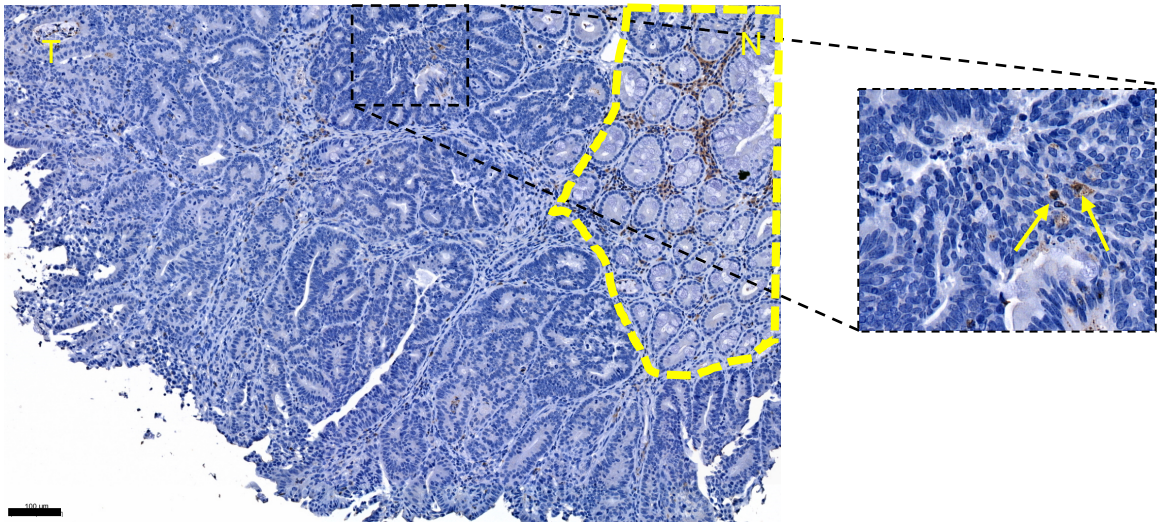

Figure 13. Representative FoxP3 staining (brown) in a tumour sample from small intestine from the Lrig1$^{CreERT2/+}$;Apc$^{flox/+}$ mouse model. Scale bar, 100 µm. The zoom-in image was taken at an 4x amplification. N- Normal tiisue adjacent to the tumour site. T- tumour site.

4.1.4. RNA extraction from CD4$^+$ T$_{eff}$ cells and Tregs sorted from tumour and blood cell suspensions

In order to accomplish the main goal of this dissertation, is pivotal to obtain a pure population of CD4$^+$ T$_{eff}$ cells and Tregs, in order to avoid contamination in the TCRβ clonotypic repertoire. For that reason, these populations were isolated from tumour samples by cell sorting in flow cytometry.

The gating strategy used to sort the populations of interest is based on Figure 6A (both for blood and tumour samples). Briefly, among viable cells, CD4$^+$ T cells were selected based on expression of CD3 and CD4 cell surface markers. Afterwards, from that population, CD4$^+$ T$_{eff}$ cells were established as the ones with lack of FoxP3 expression, whereas Tregs were

sorted from the FoxP3^{+}CD25^{+} population. Figure 14 shows a representative simplified gating strategy used to sort the populations of interest.

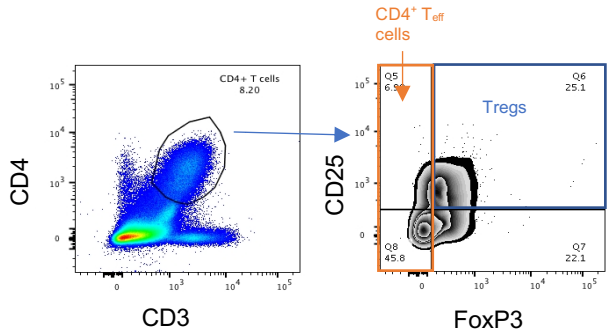

Figure 14. Representative gating strategy (simplified) to sort Tregs and CD4^{+} T$_{eff}$ cells from Lrig1$^{CreERT2/+}$;Apc$^{flox/+}$ tumour and blood samples. Among CD4^{+} T cells, CD4^{+} T$_{eff}$ cells were sorted based on lack expression of FoxP3 marker whereas Tregs were selected based on expression of CD25 and FoxP3.

Sorted cells were collected in Lysis Buffer (MagMAX™ mirVana™ Total RNA Isolation Kit) and RNA extraction was performed immediately after, in order to preserve the RNA quality. RNA quantification and quality analysis were determined using the 2100 Bionalyzer Instrument. Tables 2 and 3 summarise the number of CD4^{+} T$_{effs}$ and Tregs sorted cells from tumours and blood samples, respectively, as well as the RNA yield and RIN, to quantify the RNA integrity (from 1 (very fragmented) to 10 (undamaged RNA)) obtained for each sample. As can be observed, the amount of Treg cells fluctuates among the different samples, as well as the number of CD4^{+} T$_{eff}$ cells, showing the heterogeneity of quantity and percentage of tumour-infiltrating immune cells between animals. It is also possible to observe that RIN was very low in all samples. Moreover, the RNA quantification was not proportional with the number of cells previously sorted.

Table 2. Number of sorted cells for each substet of CD4^{+} T cell population from Lrig1$^{CreERT2/+}$;Apc$^{flox/+}$ tumours samples. The RNA yield and correspondent RIN value of each population is also presented.

Animal ID	Subset of CD4^{+} T cells	Number of sorted cells	RNA yield (pg/µl)	RIN
218FD	CD4^{+}T$_{eff}$ cells	11863	90	2
	Tregs	6270	48	1
180FDETD	CD4^{+}T$_{eff}$ cells	14609	291	2.5
	Tregs	2088	199	2.3
272FDE	CD4^{+}T$_{eff}$ cells	7282	208	2.5
	Tregs	13251	610	2.5
264FD	CD4^{+}T$_{eff}$ cells	24219	1090	2.5
	Tregs	84254	2424	2.3
299TD	CD4^{+}T$_{eff}$ cells	12729	74	2.5
	Tregs	4255	67	1.4
229FDTD	CD4^{+}T $_{eff}$ cells	16410	169	2.5
	Tregs	4345	122	2.4
357FDTD	CD4^{+}T$_{eff}$ cells	16832	154	2.5
	Tregs	30889	35	1.5

Table 3. Number of sorted cells for each substet of CD4+ T cell population from Lrig1$^{CreERT2/+}$;Apc$^{flox/+}$ blood samples. The RNA yield and correspondent RIN value of each population is also presented.

Animal ID	Subset of CD4+ T cells	Number of sorted cells	RNA yield (pg/µl)	RIN
272 FDE	CD4+T_{eff} cells	21690	616	2.5
	Tregs	1663	71	1.2
299TD	CD4+T_{eff} cells	94333	884	1.1
	Tregs	7924	34	2
229FDTD	CD4+T_{eff} cells	327755	820	2.5
	Tregs	14259	69	2.6
357FDTD	CD4+T_{eff} cells	101623	631	2.5
	Tregs	5943	31	2

4.1.5. Sequencing of TCRβ clonotypes of CD4+ T_{eff} cells and Tregs from tumour and blood samples

The best samples were selected for TCRβ sequencing in terms of RNA yield and quality. Also, the possibility of having blood samples from the same animal was considered, as this parameter could provide extra information about the conversion site of circulating Tregs and tiTregs.

For this reason, samples from the animals 272FDE, 229FDTD and 264FD were selected. In Figures 15 A and B are a representative classification of the obtained reads, where they are classified as productive reads, rescued productive reads, unproductive reads and off-target reads. This result allowed us to acknowledge if the frequency of total productive reads, constituted by productive reads plus rescued productive reads, was big enough to represent the population of tumour-infiltrating lymphocytes. In all samples, the percentage of total productive reads in the overall number of reads ranged between 0.9 and 5.9%, exposing the inefficient representation of lymphocyte population in our tumour and blood samples. As can be observed in Figure 16, the number of total productive reads was very low. Despite this, the total number of productive reads was not statistically significant among the sorted populations (Tregs and CD4+ T_{eff} cells), meaning that they received a comparable coverage between them (Figure 16). Then, we analysed the TCRβ repertoire of CD4+T_{eff} cells and Tregs from blood and tumour samples (Figure 17). Each dot in Figure 17 represents the presence of at least one clonotype for that specific CDR3 length and V segment. The diversity of the TCR clonotypes was achieved by the distribution of dots in the CDR3 length and the V region and by colour dots (dark green dots represent more TCRβ clonotypes with the same V-CDR3 length, whereas white dots represent less TCRβ clonotypes with the same V-CDR3 length). The frequency of V-CDR3 length is symbolized by the size of dots, with bigger dots representing more frequent clones.

The number of clones sequenced from both populations of interest ranged from 10 to 102. Then, we observed the diversity and frequency of TCR clonotypes in each sample. Due to the low number of clonotypes, some samples show a small diversity of TCRβ clonotypes and not distributed in all V regions (Figure 17B and 17D). In contrast, others show a huge diversity of TCRβ clonotypes not only in specific V regions with the same CDR3 length (green dots) but also distributed in more segments in variable region (Figure 17A and 17C). In most of the cases, the frequency of clones was bigger in TCRβ clonotypes with the same CDR3 length (green dots) instead of a single TCR clonotype (white dots).

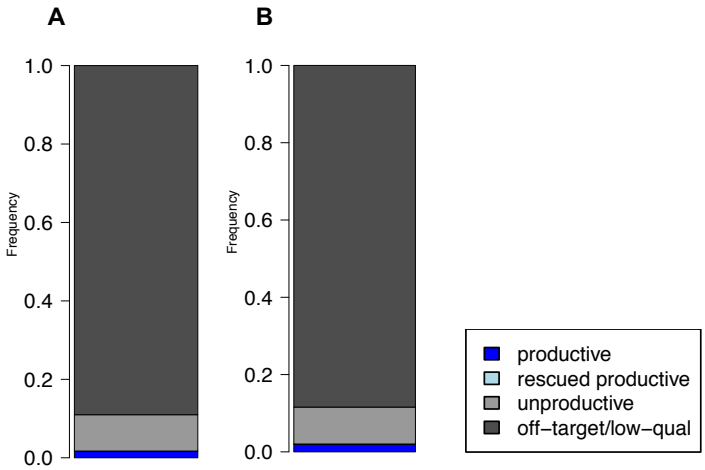

Figure 15. Representative image of reads classification after sequencing of TCRβ of CD4$^+$ T_{eff} and Tregs samples from Lrig1$^{CreERT2/+}$;Apc$^{flox/+}$ tumours. The productive and rescued productive reads are the ones analyzed by the sequencer. (A) Read classification in Treg sample from a pool of tumour; (B) Read classification in CD4$^+$ T_{eff} cells from a pool of tumours formed.

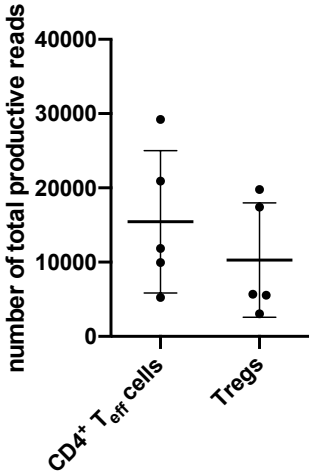

Figure 16. Number of total productive reads obtained after sequencing of TCRβ sequences from Lrig1$^{CreERT2/+}$;Apc$^{flox/+}$ tumour and blood samples sorted lymphocytes. Each dot represents the number of total productive reads for each sample of CD4$^+$$T_{eff}$ cells and Tregs sequenced (n=5). Two tailed Mann-Whitney test was used for statistical analyses. No significant differences were observed between total productive reads from both populations, ($p>0.05$). Error bar is for standard deviation.

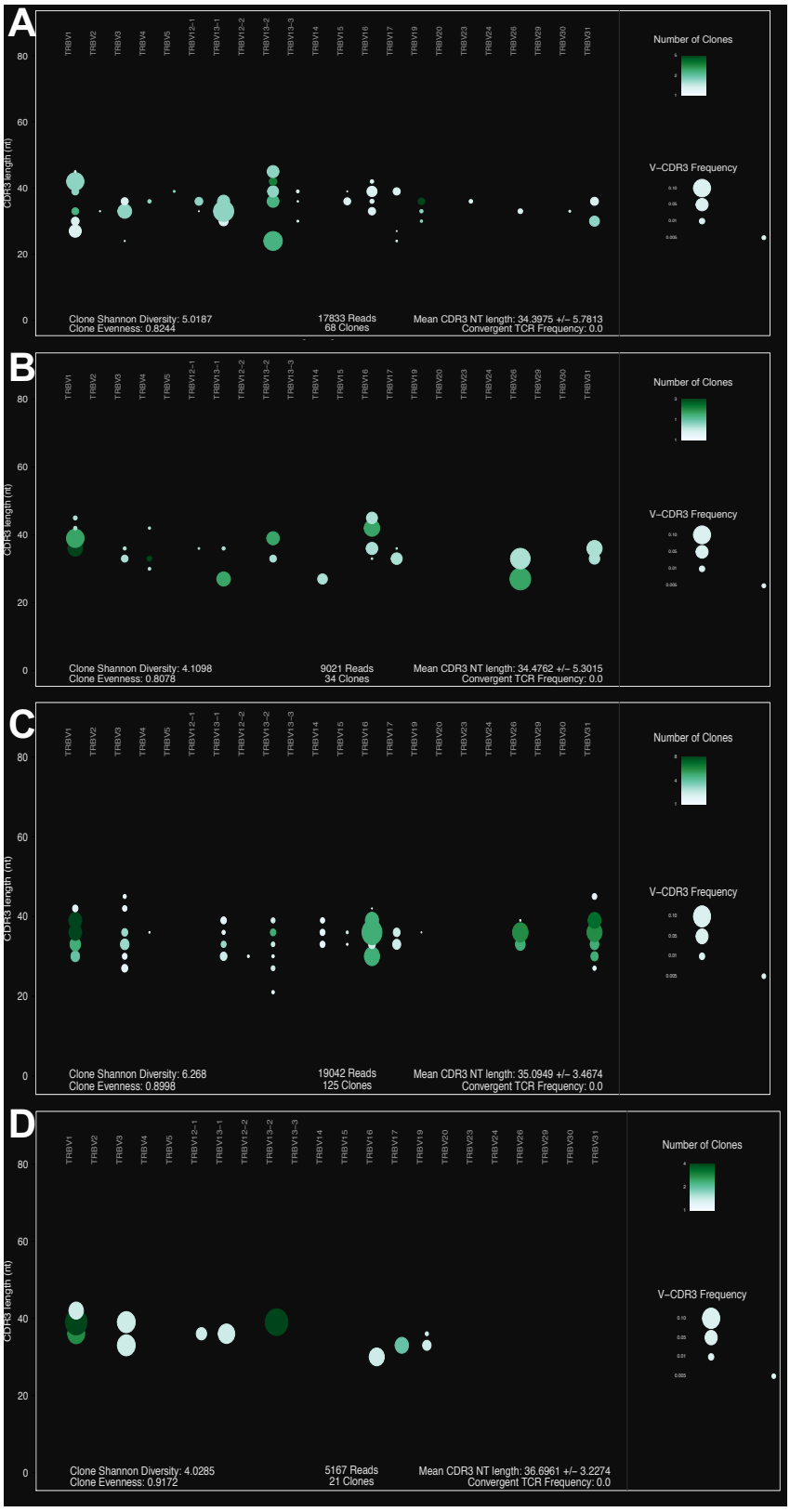

Figure 17. Representative distribution of TCRβ clonotypes present in the sorted populations from Lrig1$^{CreERT2/+}$;Apc$^{flox/+}$ tumour and blood samples.

Representation of TCRβ clonotypes present in (A)/(B) Tregs/ CD4^{+} T_{eff} cells population in tumour and (C)/(D) Tregs/ CD4^{+} T_{eff} cells in blood from 272FDE mouse; The sequences are distributed by their CDR3 length, and each dot represents the presence of clones for that specific V segment and CDR3 length. The diversity of clones in each dot is represented by colour (from white to dark green) and the frequency by size (bigger dots represent the presence of more frequent V-CDR3 sequences).

4.1.6. Comparison between the TCRβ sequences of CD4$^+$ T_{effs} with Tregs in tumour *vs* blood samples

After sequencing the TCRβ repertoire from CD4$^+$ T_{eff} cells and Tregs, we next compared the sequences from both populations to infer about the origin of tiTregs. By comparing the CDR3 region in the TCRβ sequence between the populations of interest, we observed that a small proportion of the sequences overlap between CD4$^+$ T_{eff} cells and Tregs collected from tumour samples (Figure 18). Only in tumour samples from 264FDTD and 272FDE animals were observed the presence of 3 TCRβ clonotypes that shared the same TCRβ sequence between CD4$^+$ T_{effs} and Tregs, showing that most of Treg clonotypes present at the tumour site have a central origin.

Moreover, we also compared the TCRβ sequences from these populations in blood *versus* tumour samples (Figure 19). In blood samples from 229FDTD mouse, there were 7 TCRβ sequences shared between Tregs and CD4$^+$ T_{eff} cells (Figure 19A). Figure 19B shows one TCRβ clonotype shared by tiTregs with Tregs in blood and another TCRβ clonotype shared by Tregs in blood and both CD4$^+$ T_{eff} populations, in blood and in tumour.

In addition, 3 TCRβ sequences overlapped between the TCRβ repertoire of CD4$^+$ T_{eff} population with TCRβ repertoire of Tregs population from blood samples and other 3 TCRβ sequences were shared in Tregs and CD4$^+$ T_{eff} populations from tumour. Regarding these 3 TCRβ clonotypes, the ranking of frequency of them in tiTreg population were 13rd ,16th and 53th.

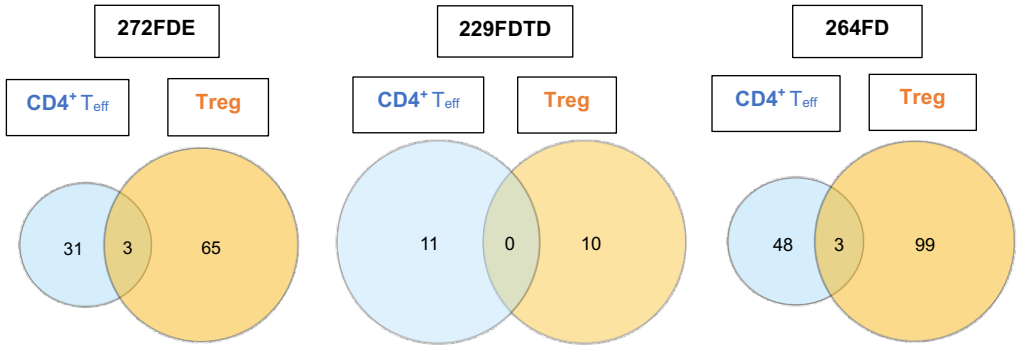

Figure 18. Comparision of TCRβ sequences between tumour-infiltrating CD4$^+$ T_{eff} cells and Tregs collected from Lrig1$^{CreERT2/+}$;Apc$^{flox/+}$ mice. The overlapp region between circles present the number of TCRβ sequences shared by both populations.

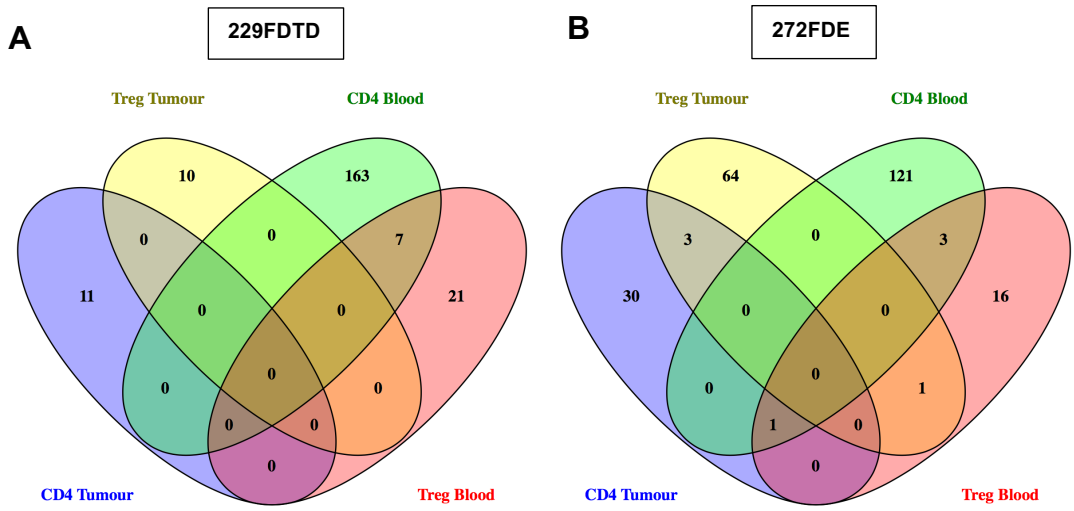

Figure 19. Comparison of the TCRβ sequences between CD4$^+$ T_{eff} cells and Tregs from blood and tumour samples collected from Lrig1$^{CreERT2/+}$;Apc$^{flox/+}$ mice. (A) Comparison between CD4$^+$$T_{eff}$ cells and Tregs in tumour and blood samples from 229FDTD mouse; (B) Comparison between CD4$^+$$T_{eff}$ cells and Tregs in tumour and blood samples from 272FDE mouse. Blue and yellow circles indicate the number of CD4$^+$ T_{eff} cells and Tregs clonotypes sorted from tumours, respectively. Green and red circles show the number of TCRβ clonotypes from CD4$^+$$T_{eff}$ and Tregs cells sorted from the blood, respectively.

4.2. FoxP3$^{eGFP.DTR.Luci}$ mouse model

4.2.1. Evaluation of tumour growth kinetics

Due to the poor number of total productive reads obtained from the neoplastic and blood samples collected from Lrig1$^{CreERT2/+}$;Apc$^{flox/+}$ mice, we decided to sort cells from tumours of a different mouse model, the FoxP3$^{eGFP.DTR.Luci}$ mice. In this model, all FoxP3$^+$ cells express the enhanced green fluorescence protein (eGFP), which allow their identification and sorting without the need to fix or permeabilize them.

Six animals (4 females and 2 males) were subcutaneously inoculated with 1x10^6 MC38 cells (in 100 µl of saline solution) for tumour development. Tumour growth kinetics is presented in Figure 20 showing that only three out of the six mice developed a visible tumour. Moreover, the tumour growth rate was very different among animals, with the 7FE mouse presenting the highest tumour growth rate, whereas the 9TD mouse had the lowest.

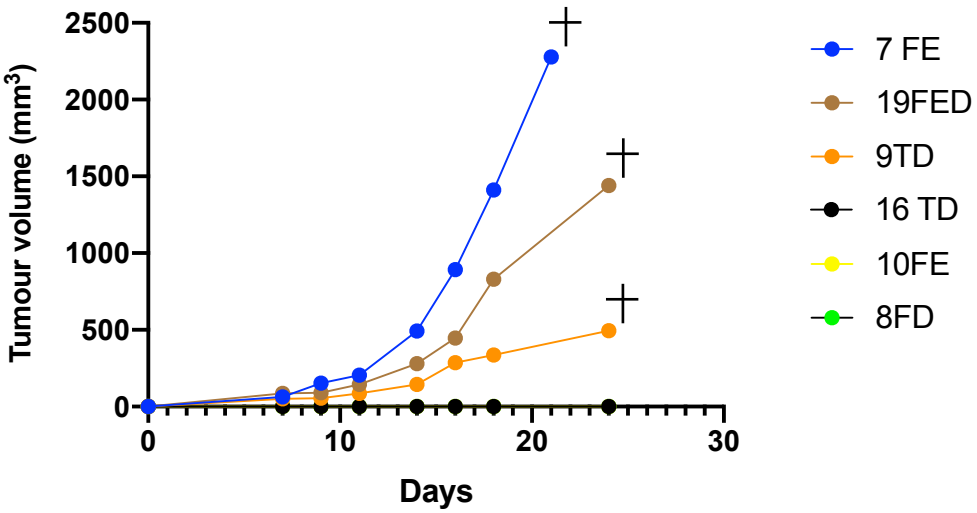

Figure 20. Tumour growth kinetics in FoxP3$^{eGFP.DTR.Luci}$ mice after subcutaneous inoculation with MC38 cells. One million cells were inoculated subcutaneously and the tumour growth was monitored every 2-3 days . Tumour volume is presented in mm^3. The cross symbol represents the day of euthanasia.

4.2.2. Immune cells composition at the tumour site

The animals that developed a visible tumour were euthanized between 20 and 30 days after inoculation or when tumour reached 2000 mm^3. Subsequently, tumours were collected followed by digestion and immunophenotyping by flow cytometry to characterise the immune composition of the MC38-derived subcutaneous neoplastic lesions. For that, Tregs and CD25$^-$FoxP3$^+$ T cells were analysed accordingly to the gating strategy presented in Figure 21, and the percentage of these populations among all viable cells was quantified (Figure 22).

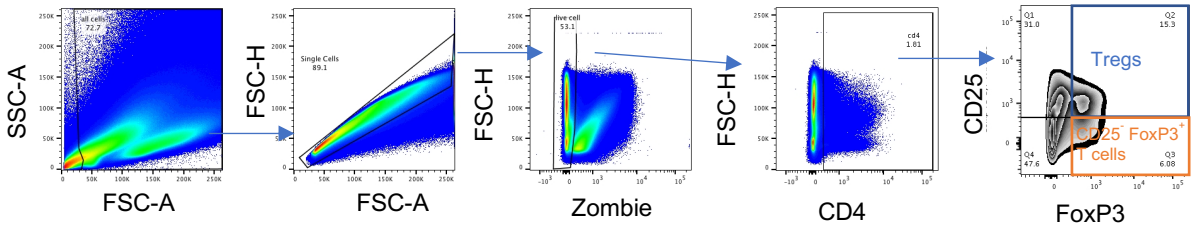

Figure 21. Gating strategy used for the analysis of tumour-infiltrating lymphocytes in FoxP3$^{eGFP.DTR.Luci}$ mice by flow cytometry. Among viable cells, CD4$^+$ cells were gated by staining of CD4. Among these, the gating for Treg cells was performed in the FoxP3$^+$ and CD25$^+$ population. CD25$^-$FoxP3$^+$ T cells were also selected, based in absence of CD25 expression and strong staining for FoxP3.

The results show that Treg cells are present in these tumours in a proportion of about 0.2% of all viable cells, although having some variability among tumour samples (Figure 22). Interestingly, the presence of a population of CD25$^-$FoxP3$^+$ T was also detected, comprising around 0.1% of the total number of viable cells. No significant differences were observed in the percentage of both populations among viable cells.

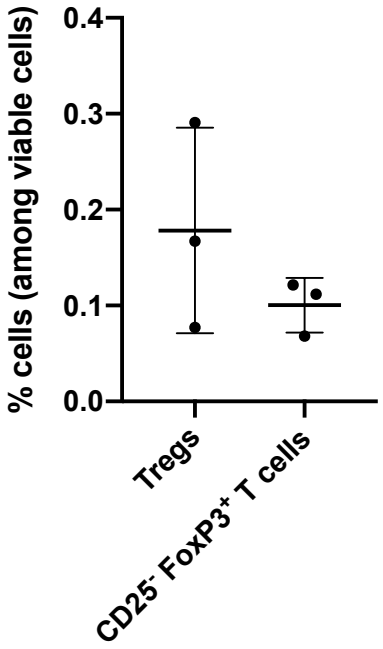

Figure 22. Immune composition of MC38-derived tumours collected from FoxP3$^{eGFP.DTR.Luci}$ animals analysed by flow-cytometry. Each dot represents the percentage of immune cells quantified using a tumour sample from a different animal. Two-tailed Mann-Whitney test was used for statistical analyse. No significant differences between groups ($p>0.05$) were observed. Error bars stands for standard deviation.

4.2.3. RNA extraction from CD4$^+$ T$_{eff}$ cells and Tregs sorted from MC38-derived tumours

The number of sorted CD4$^+$T$_{eff}$ cells and Tregs is shown in Table 4. The number of Tregs sorted seemed to be proportional with tumour size on euthanasia day (Figure 20), whereas the number of CD4$^+$ T$_{eff}$ cells was more homogenous among samples, despite their differences in terms of size. After sorting these populations, total cell RNA was extracted and quantified both for yield and quality (integrity) in the 2100 Bioanalyzer Instrument (Table 4).

Table 4. Numbers of sorted cells for each substet of CD4$^+$ T cell population from MC38-derived subcutanous tumours. The RNA yield and correspondent RIN to each population is also presented. (N/A-non aplicable)

Animal ID	**7FE**		**19FED**		**9TD**	
Type of cell	CD4$^+$T$_{eff}$ cells	Tregs	CD4$^+$T$_{eff}$ cells	Tregs	CD4$^+$T$_{eff}$ cells	Tregs
Number of cells	36039	1027	37215	820	39099	316
RNA yield (pg/µl)	672	160	678	38	395	22
RIN	3.9	3.9	2.5	2.5	2.3	N/A

4.2.4. Sequencing of TCRβ clonotypes of CD4$^+$ T_{eff} cells and Treg cells and comparison of their TCRβ repertoire

The same sequencing approach as described before for the Lrig1$^{CreERT2/+}$;Apc$^{flox/+}$ mouse model samples was performed. Although, due to technical issues, only one (7FE) out of the three samples collected from the FoxP3$^{eGFP.DTR.luci}$ mice was possible to sequence. From the other 2 samples, no reads were detected for the Treg population and therefore we were not able to use the data from CD4$^+$ T_{eff} sequencing to achieve our aim. The classification of reads obtained for the 7FE sample is presented in Figure 23. As can be observed, we were able to obtain a total of 63% of productive reads for CD4$^+$ T_{eff} cells and 53% for Tregs, plus 2.7 and 3% of rescued reads, respectively. The diversity and frequency of TCRβ clonotypes present in each sample is illustrated in Figure 24.

Figures 24A and 24B show the presence of 243 TCRβ clonotypes for the Tregs population and 1016 TCRβ clonotypes for the CD4$^+$ T_{eff} population, respectively. The distribution of TCRβ clonotypes in both populations indicated a huge diversity based on the number of dots presented in a wide range of variable region and the presence of green dots in certain CDR3 length. Comparing the distribution of both populations, the TCRβ repertoire of CD4$^+$ T_{eff} cells appears to be similar with TCRβ repertoire of Tregs. None of Figures 24A and 24B indicate a single TCRβ clonotype with a high frequency (big white dots) whereas TCRβ clonotypes with the same CDR3 length have a high V-CDR3 frequency.

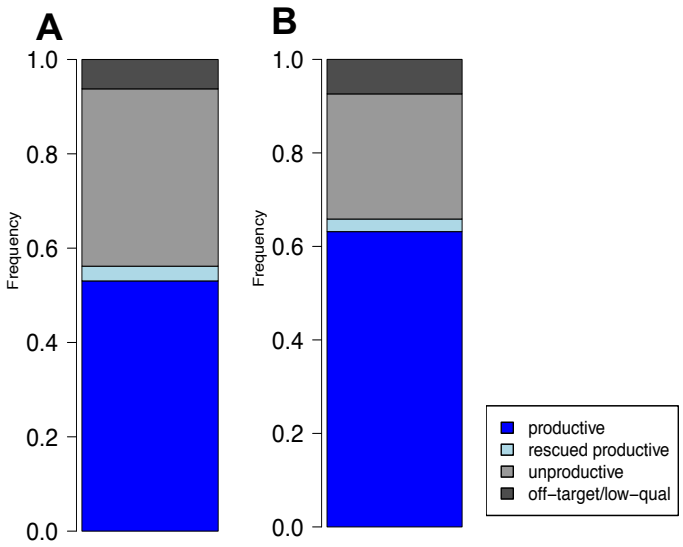

Figure 23. Read classification of sequencing in Tregs and CD4$^+$ T_{eff} population from MC38-derived subcutaneous tumour. The productive and rescued productive reads are the ones analyzed by the sequencer. (A) Read classification in Treg sample from MC38-derived subcutaneous tumours. (B) Reads classification of CD4$^+$ T_{eff} cells from MC38-derived subcutaneous tumour.

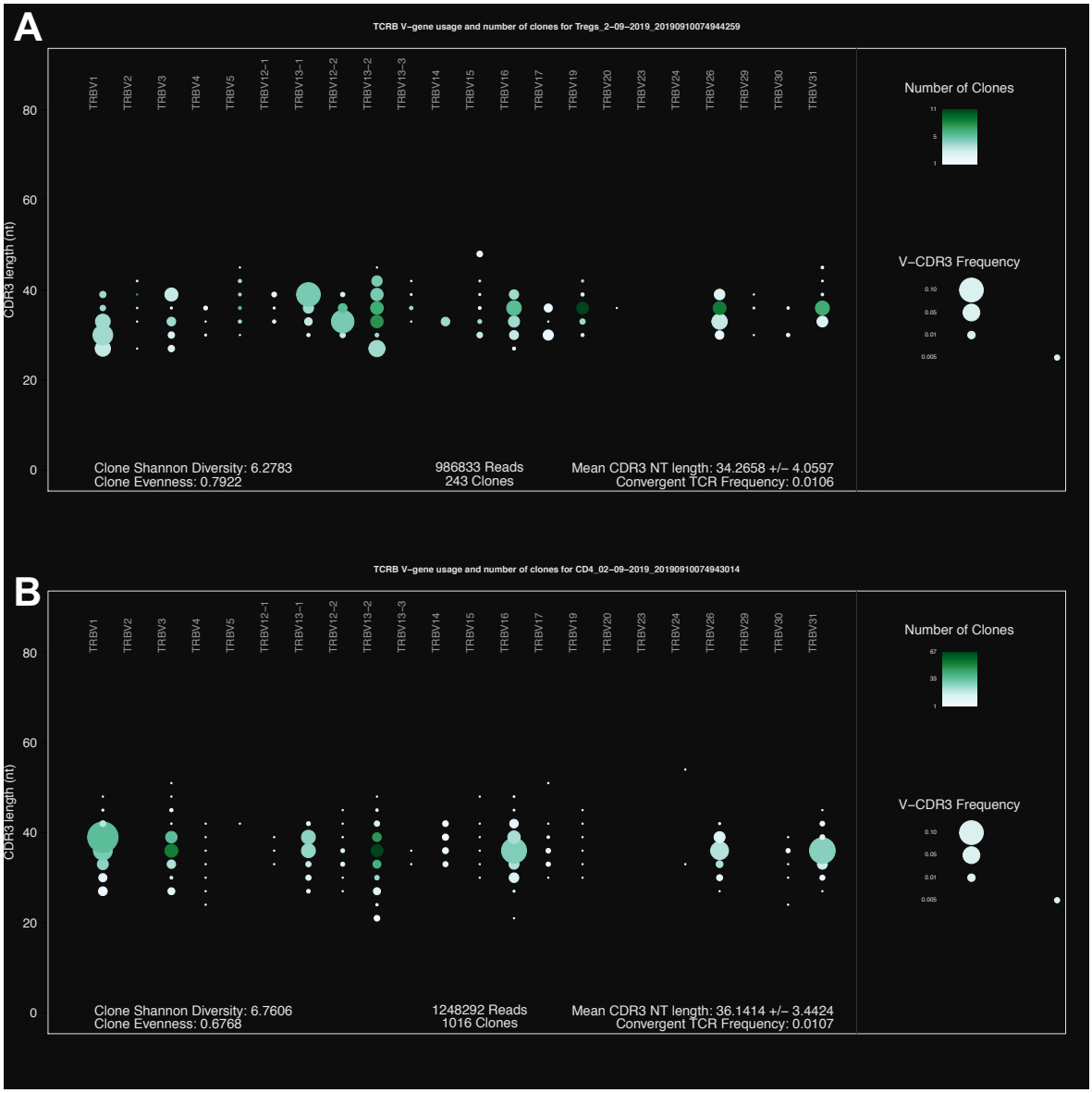

Figure 24. Distribution of TCRβ clonotypes present in the sorted populations from the MC38-derived subcutaneous tumours. (A) TCRβ clonotypes distribution of Tregs and; (B) $CD4^+$ T_{eff} cells. The sequences are distributed by their CDR3 length, and each dot represents the presence of clones for that specific V segment and CDR3 length. The diversity of clones in each dot is represented by colour (from white to dark green) and the frequency by size (bigger dots represent the presence of more frequent V-CDR3 sequences).

Finally, we analysed the sequencing data and compared the CDR3 of the TCRβ sequence between both populations to understand the origin of Tregs sorted from MC38-derived tumours (Figure 25). We observed that 102 TCRβ clonotypes are shared between these two populations, suggesting that, based on the CDR3 region from the TCRβ, there are 102 Treg clones peripherally converted from $CD4^+$ T_{eff} cells.

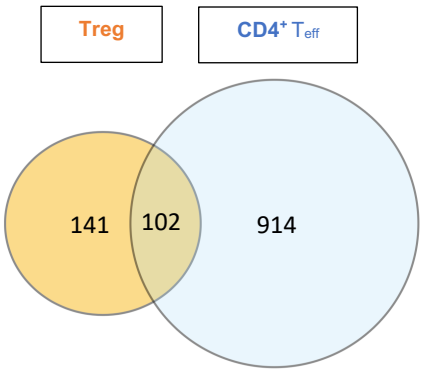

Figure 25. Comparision of TCRβ sequences between tumour-infiltrating CD4$^+$ T$_{eff}$ cells and Tregs from a MC38-derived subcutaneous tumour developed in FoxP3$^{eGFP.DTR.Luci}$ mice. The overlapp region between circles present the number of TCR sequences shared by both populations.

4.3. Comparison between TCRβ repertoire of tumour-infiltrating CD4$^+$ T$_{eff}$ cells and Tregs in different animals

Finally, we assessed if tumour-infiltrating CD4$^+$ T$_{eff}$ or tiTregs could share the same TCRβ clonotypes in different animals, by comparing all samples amongst each other (from both Lrig1$^{CreERT2/+}$;Apc$^{flox/+}$ and FoxP3$^{eGFP.DTR.Luci}$ mice). The results from this comparison are represented in Figures 26A and 26B, for CD4$^+$ T$_{eff}$ cells and Tregs, respectively. Tumour-infiltrating CD4$^+$ T$_{eff}$ cells did not show any overlap between different animals in terms of CDR3 region of TCRβ, whereas in the case of the Treg clonotypes, only one was shared between tiTregs from the animals 264FD and 272FDE. Despite this TCRβ clonotype shared by these Tregs populations, this T cell clone had a low frequency in both populations, less than 0.1 %. This data expose that the response/recruitment of cells to the tumour site was realized by diverse T cell clonotypes in different animals.

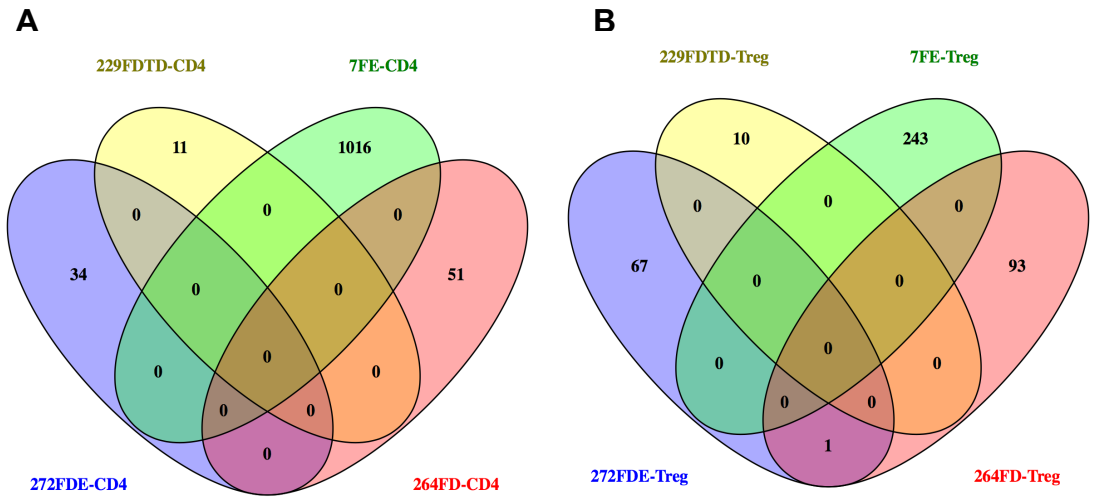

Figure 26. Comparison of the TCRβ sequences between CD4$^+$ T_{eff} cells and Tregs from tumour samples collected from both Lrig1$^{CreERT2/+}$;Apc$^{flox/+}$ and FoxP3$^{eGFP.Luci.DTR}$ mice. Comparison between (A) CD4$^+$ T_{eff} and (B) Treg populations gathered from different animals. Red and green circles show the number of TCRβ clonotypes from 264FD and 7FE mice, respectively. Yellow and blue circles present the number of TCRβ clonotypes identified in 229FDTD and 272FDE tumour samples.

5. Discussion

Immunotherapy with immune checkpoint blockers has changed the cancer treatment landscape over the last years. However, despite remarkable clinical results, about 80% of patients do not respond to this type of therapy [22]. This suggests the existence of alternative mechanisms of escape to cancer immune response.

The ability of Tregs to infiltrate neoplastic lesions has already been proven, contributing to the increased tolerance from the immune system towards tumour cells in the majority of cases [86, 87]. Moreover, in most cancer types, the presence of Tregs at the tumour site is associated with a worse prognosis for patients' overall survival [86]. Despite their presence being well documented, little is known about the origin of tiTregs – they can be derived from the thymus (central origin) or from the peripheral conversion of $CD4^+$ T cells (peripheral origin). Only two markers, NRP1 and Helios, have been proposed to distinguish Tregs regarding their origin [81]. However, their use for Treg differentiation has been questionable with some articles showing that Helios is a marker of cell activation in presence of antigens and that the TCR repertoire of $NRP1^{high}$ and $NRP1^{low}$ was similar, suggesting that they share the same lineage [81, 85].

Taking this into consideration, to date, there is no specific marker to distinguish these Treg lineages. For this reason, the main goal of this dissertation is to elucidate the origin of tiTregs.

To achieve this aim, an inducible and conditional mouse model of intestinal/colonic tumorigenesis, the $Lrig1^{CreERT2/+}$;$Apc^{flox/+}$, was used [100]. This model represents more faithfully the natural occurrence of tumours in the intestinal/colon tissue by loss of one *Apc* allele in $Lrig1^+$ cells.

We started the work by characterising the mouse model. To do so, the location of tumours, number and size were registered. Despite the development of tumours along the small intestine and colon as previously documented, the number and typical localization of tumours were altered compared to what was reported in the original publication by Powel *et al.,* who kindly gifted us the mice [100]. The authors reported an average around 40 tumours per animal, being most of them in the jejune region. However, the maximum number of tumours detected by us was of 33, with an average of 6.5 per animal. Moreover, the location of the GI tract with the highest number of tumours detected was in the proximal part of small intestine (duodenum), with an average of 4.7 tumours per mouse. One possible explanation for this phenomenon can be related with the mice microbiome, as it will be different among distinct animal facilities. Some reports have shown that differences in microbiome lead to different growth kinetics and number of tumours, especially in the intestinal tissue, where the presence of certain species of bacteria could favour the process

of carcinogenesis [102-104]. Another explanation can be related to the process of mice rederivation in our animal facility, since the animals lost their C57BL/6 background to sv129, which might altered the susceptibility of these animals to develop tumours [105].

Having characterised the mouse model, we next analysed the collected tumours to confirm the presence of tumour-infiltrating Tregs. For that, the immune composition of a pool of tumours (representing one sample) collected from different Lrig1$^{CreERT2/+}$;Apc$^{flox/+}$ mice was analysed by flow cytometry. Cells were stained with anti-CD3, anti-CD4, anti-CD25 and anti-FoxP3 antibodies to distinguish between CD8$^+$ T, CD4$^+$ T and Treg populations, and may understand if the percentages of these cells in the immune infiltrate of these samples is homogenous between mice and to evaluate the presence of tiTregs. Interestingly, a population of CD25$^-$FoxP3$^+$ T cells that we did not expect to observe was also detected in some of these samples, and in some cases, in a higher percentage than the Treg population. The origin or function of this population is not well understood so far, but some authors have claimed that it constitutes a reservoir for Treg generation that can upregulate CD25 expression upon homeostatic expansion and therefore, activated Tregs [106]. Other reports described that this population can lose the FoxP3 expression and become T helper cells, or that CD25$^-$FoxP3$^+$ T cells turn out to be immunosuppressive in aged mice [107-109]. Two possible explanations for the presence of this type of inactivated Tregs are correlated with a) the suppression of Tregs activity by tumour influence or b) the recruitment of cells that have not interacted with an antigen yet and will be converted into Tregs after expressing CD25. However, these two hypotheses are speculative with little support given by the literature so far [65, 106, 108].

The analysis of the immune composition showed no statistically significant differences between pairs of CD4$^+$ T cells and CD8$^+$ T cells plus Tregs and CD25$^-$FoxP3$^+$ T cells. This data indicates that these tumours have a similar proportion of the CD8$^+$ T cells and CD4$^+$ T cell populations (<5%), and the same is true for the other analysed populations (~1%). Wang *et al.* showed that, in human cancers, there is a better prognosis in overall survival and progress free survival rates in triple-negative breast cancer patients that had a ratio of CD4/CD8 above 1 [110]. Additionally, a study by Shah and co-workers have determined that a CD4/CD8 ratio below 1 and the presence of high infiltration of Tregs are associated with worst prognosis in squamous cell carcinoma of the cervix [111]. Despite these observations, in tumours from Lrig1$^{CreERT2/+}$;Apc$^{flox/+}$ mice we detected a ratio of CD4/CD8 around 1, and they are not considered to be highly infiltrated by Tregs (only 1% of all viable cells in tumour). Thus, our results could not be correlated with the previous reports.

The presence of tiTregs in the neoplastic lesions was also confirmed by immunohistochemistry. Even though it was possible to observe a high density of staining in the lesion periphery (normal tissue adjacent to the tumour tissue), small amounts of tiTregs

in intratumoural site were detected. This could be responsible for the formation of a favourable tumour microenvironment, leading to the suppression of the immune response in the peripheric region of tumour.

Due to the relative low amount of immune infiltration in these tumours and the fact that they have relatively low dimensions, the number of cells that we could sort from these samples was very low (Table 2 – Results Section). Therefore, the quantity of RNA was predictable to be also lower. Moreover, due to the necessity to fix and permeabilize cells for the intracellular staining of FoxP3, the RNA integrity was compromised [112, 113]. Also, the process of tissue digestion and immunophenotyping lead to cell stress and may result in the activation of endogenous RNases, contributing for less quantity and quality of RNA and even cell death.

Because these issues, the samples used for TCRβ sequencing were not ideal, although we have chosen the ones with the best scores in terms of RNA quantity and integrity. To assess if our sequencing data was representative of the whole sample, the amount of the total productive reads was analysed. Unfortunately, the number obtained was very low, as somehow expected due to the fixation step – not only it affects RNA integrity, as it can affect the amplification step needed for sequencing [113]. From our experience, a minimum of 20% of total productive reads are necessary to have a good representation of all sequences in the sample (unpublished data). For this reason, the results obtained from this sequencing do not totally represent the diversity of TCRβ clonotypes present in tumour and blood samples from $Lrig1^{CreERT2/+}$;$Apc^{flox/+}$ mice. Regardless, the number of productive reads from both $CD4^+$ T_{eff} and Tregs populations was not significantly different and thus, we assume that the sequencing coverage for both populations was similar, being possible to compare them.

After preliminary analysis of the sequenced number of reads, we evaluated the frequency and diversity of TCRβ clonotypes from $CD4^+$ T_{eff} cells and Tregs present in both samples (blood and tumour). Due to the low number of reads sequenced, some samples had low number of TCRβ clonotypes detected and the T cell clonotypes had preferentially the same CDR3 length and V segment than a similar distribution in all segments of V region. Both tumour-infiltrating Tregs and $CD4^+$ T_{eff} cells from 229FDTD mouse are an example of low quantity of TCRβ clonotypes, which had 10 and 11 TCRβ clonotypes, respectively. At the tumour site, we expected to observe a high frequency of some clonotypes, indicating a specific response to locally expressed antigens that would be represented by bigger and white dots (Figure 17 from results section). However, most dots with higher frequency of V-CDR3 are composed by many clonotypes, which represent the sum of all T cell clonotypes with the same CDR3 length and specific V segment. But if we want to evaluate the specific

tumour response, we need to focus more in the amino acid sequence and their structure because different TCRβ clonotypes can form the same protein.

We next compared the TCRβ sequences obtained from $CD4^+$ T_{eff} cells *versus* Tregs to achieve the proposed goal of this dissertation, which is to understand the origin of tiTregs. The results from that comparison clearly show that most of tiTreg clonotypes did not share the same CDR3 region of TCRβ sequences from $CD4^+$ T_{eff} cells. Therefore, we can suggest that the majority of Treg clonotypes present at the tumour site have a central origin, which indicates that central tolerance plays a crucial role in tumour development. Perhaps this result could be explained by the expression of self-antigens by tumour cells, since they were transformed from normal cells, although we could not rule out the hypothesis of other mechanisms of transport of tumour-derived neoantigens to the thymus [52]. However, we need to be careful with these results because the sequencing was not fully representative of both populations in tumour sample, based on the reads classification regarding low quantity and quality of RNA.

Regarding peripheral Tregs, an additional question remains in our mind that is if this conversion happens at the tumour site and is stimulated by cancer cells, or if it occurs in other locations caused by a peripheral tolerance and not related with cancer disease. To answer this question, we compared the populations of interest ($CD4^+$ T_{eff} cells and Tregs) in tumour *versus* blood. We did not observe any overlap between the TCRβ repertoire present in these two samples from 229FD mouse. The data obtained with the samples collected from the 272FDE mice show one TCRβ clonotype of tiTregs shared with circulating Tregs and another TCRβ clonotype that is shared by Tregs in blood and $CD4^+$ T_{eff} from both samples (blood and tumour). Additionally, in the same samples from 272FDE mouse, 6 Treg clonotypes had the same TCRβ sequence of $CD4^+$ T_{eff} clones, meaning that they were converted from these cells. Interestingly, 3 TCRβ clonotypes were shared between Tregs and $CD4^+T_{eff}$ population from the blood, so they are probably originated by a process of peripheral tolerance without being related with the tumour, whereas the other 3 tiTreg clonotypes shared with the $CD4^+$ T_{eff} cells from the tumour probable result from the local conversion of these cells. The local conversion of Treg cells in neoplastic lesions could be explained by the presence of tumour-related neoantigens and by expression some molecules such as TGF-β, which may trigger this process [114].

To surpass the technical limitations of this initial study regarding the necessity for fixation and permeabilization of cells and consequently loss of RNA integrity, we decided to test another animal model to determine the origin of tiTreg, the $FoxP3^{eGFP.DTR.Luci}$ mice. This mouse is a BAC transgenic model in which a construct composed by eGFP, DTR and luciferase genes was inserted in the third exon of the *FoxP3* gene and randomly integrated

into the genome [101]. As a result, ~90% of FoxP3$^+$ cells from these mice are eGFP positive and can be detected by flow cytometry without the need for antibody labelling. For tumour development, the colorectal adenocarcinoma-derived cell line (MC38) was subcutaneously injected, as these animals do not have an inducible system to development intestinal/colon tumours as the Lrig1$^{CreERT2/+}$;Apc$^{flox/+}$ mice. From the 6 mice initial injected with MC38 cells, only 3 developed a visible tumour. Previous work from our group in using MC38 cells for subcutaneous inoculations in mice had shown that the immune system can recognise these cells as non-self in some cases, due to the characteristic alterations of a cell line, contributing to its elimination (unpublished data). This could also be related with low cell viability at the time of injection or a technical difficulty in the subcutaneous injection.

The animals were euthanized between 20 and 30 days after inoculation or when tumour reached 2000 mm^3. Afterwards, each tumour was collected and analysed for its immune composition. Herein, we only evaluated the presence of Tregs and CD25$^-$FoxP3$^+$ T cells and did not account for the CD4$^+$ T cell population. The reason for this is because the eGFP from FoxP3$^+$ cells has its emission in the same wavelength of FITC, which is the fluorochrome conjugated with the anti-CD3 antibody available in our lab, and so it could not be used. As the CD4 marker is not exclusive of CD4$^+$ T cells, since dendritic cells also express this protein, we decide to not include them in our evaluation [115]. When comparing the populations of Tregs *versus* CD25$^-$ FoxP3$^+$ T cells in these tumours, the former appears to be at higher levels, despite this difference being not statistically significant. A higher number of samples is needed to understand if this phenomenon is real and to compare this difference with tumour size on euthanasia day or tumour growth rate.

Due to the small percentage of tiTregs, the number of Tregs that we were able to sort was very low. However, a positive correlation between the number of Tregs and tumour volume was detected. This can occur because having a higher tumour mass will lead to a higher number of cells being present, including Tregs, or due to the creation of an immunosuppression microenvironment by Tregs that would increase tumour growth rate.

After analyses of the tumour-infiltrating lymphocytes and their sorting, RNA extraction and TCRβ sequencing was performed. Although we have used all samples gathered for these sequencing step (3 Treg samples and 3 CD4$^+$ T_{eff} cells collected from 3 MC38-derived subcutaneous tumours), 2 RNA samples from sorted Tregs were not sequenced because the sequencer did not recognise their barcodes. The protocol was performed twice, with a change in the barcode in the second attempt, but with the same result. The small number of cells and the low quality of RNA could be the reason for this issue. Therefore, we only analysed the pair of samples from one tumour (7FE).

The percentage of total productive reads obtained from the MC38-derived tumours was significantly higher (56-66%) when compared to what was obtained from the samples

collected from Lrig1$^{CreERT2/+}$;Apc$^{flox/+}$ mice, validating the influence of the fixation/permeabilization method in this process. With these values we are confident that the obtained data is representative of the tumour immune composition. The results obtained from sequencing confirms this idea, with a bigger distribution and higher number of TCRβ clonotypes being gathered. Despite the absence of TCRβ clonotypes with high frequency that could be reactive for a specific antigen, there are some clonotypes showing an intermediate level of frequency, indicating some clonal expansion in response to some local antigens.

Finally, to understand the origin of tiTregs in this mouse model, we compared the TCRβ sequences obtained from CD4$^+$ T$_{eff}$ cells and Tregs populations. A similar result to the one presented before was achieved, with the majority of Tregs (141 out of 243 clonotypes) having unique TCRβ sequences and therefore being considered tTregs, reinforcing the role of central tolerance in tumour development [116]. Nevertheless, the percentage of pTregs clonotypes in this mouse model, about 40% of total of tiTreg clonotypes, is higher when compared to the results obtained from the Lrig1$^{CreERT2/+}$;Apc$^{flox/+}$ mice. In the literature, there are at least two studies using tumour cell lines as a model of tumour development in mice that described the presence of Tregs conversion from CD4$^+$ T cells in tumour site but also in draining lymph node and spleen [117, 118].

We also compared the TCRβ sequences between all the different animals used in this work, to understand if there is any sequence that overlaps among the same subset of cells. Only one TCRβ clonotype was shared by two Treg populations from two Lrig1$^{CreERT2/+}$;Apc$^{flox/+}$ mice, but at a very low frequency in both cases and thus, we cannot assume that this TCRβ clonotype that is shared by both animals is tumour specific.

Regardless the results obtained from these TCRβ sequence comparisons, there are some limiting parameters that must be considered. First, our TCRβ repertoire is not totally representative of the whole repertoire of CD4$^+$ T$_{eff}$ cells and Tregs present in the Lrig1$^{CreERT2/+}$;Apc$^{flox/+}$ tumour samples. Moreover, we only sequenced the CDR3 region of the TCRβ, which is the most diverse region of this protein chain, but there is the possibility to occur punctual mutations in other regions of the TCRβ that we do not detect using this analysis. Besides, we have to take into account that the TCR is a heterodimer receptor and most of them are also composed by another chain, the TCRα, which also has a CDR3 region. Therefore, the number of clonotypes of CD4$^+$ T$_{eff}$ and Tregs that share the same TCRβ detected by sequencing can be inflated comparing with the real number of pTregs in tumour site. Despite these limitations, a recent publication by Ahmadzadeh *et al.* described similar results to those observed in this work in a variety of human cancers in terms of origin of tiTregs. They compared the TCRβ sequences of CD8$^-$FoxP3$^+$ T with CD8$^-$FoxP3$^-$ T cells

and showed that a minority of clonotypes are shared between these populations, but contrary to our findings, they detected a high frequency of overlapping TCRβ clonotypes in same subsets of $CD4^+$ T cells from blood *versus* tumours [116].

In summary, and despite important limitations of the study so far, in our models we were able to observe the presence of tiTregs, being the majority of them likely of central origin, which suggests that central tolerance is important in cancer development. However, in the subcutaneous tumour model we observe a big percentage of clonotypes to be formed in periphery showing that peripheral tolerance is also important to tumour progression.

6. Conclusion and Futures Perspectives

In this study, we proposed to achieve two aims: identify the presence of tumour-infiltrating Tregs from Lrig1$^{CreERT2/+}$;Apc$^{flox/+}$ tumours and MC38-derived subcutaneous tumours from FoxP3$^{eGFP.DTR.Luci}$ mice, and determine the origin of tumour-infiltrating Tregs based on the TCRβ repertoire of Tregs and CD4$^+$ T_{eff} cells from these two different tumour models. In the Lrig1$^{CreERT2/+}$;Apc$^{flox/+}$ tumours and the MC38-derived subcutaneous tumours, Tregs were present in tumour. The results of this work also indicate that the majority of tiTreg clonotypes do not share their TCRβ sequences with CD4$^+$ T_{eff}. clonotypes. Therefore, we can infer that tiTeg clonotypes have mostly a central origin, evidencing the important role of central tolerance in tumour development. Although in MC38 derived subcutaneous tumour has a high fraction of Treg clonotypes that had a peripheral origin evidencing the crucial role of peripheral tolerance in this tumour progression. Despite the major proportion of tiTregs being tTregs, we also demonstrated that some Treg clonotypes are locally converted, perhaps by tumour influence, through the comparison of TCRβ sequences between CD4$^+$ T_{eff} cells and Tregs in blood *vs* tumour samples.

Nonetheless, this study has some limitations such as the low number of samples, small number of tiTregs collected and low quality of RNA.

To reduce these limitations, MC38 will be subcutaneously inoculated in a higher number of FoxP3$^{eGFP.DTR.Luci}$ animals to increase the significance of the gathered data so far. Simultaneously, the Lrig1$^{CreERT2/+}$;Apc$^{flox/+}$ mouse model will be crossed with FoxP3$^{eGFP.DTR.Luci}$ mice to generate an inducible system of intestinal/colonic tumour development where all FoxP3$^+$ cells are labelled and can be easily isolated without the need for further processing. Also, we would like to sequence the TCRβ repertoire of CD25$^-$FoxP3$^+$ T cells to understand if it is more similar to the TCRβ repertoire of Tregs or CD4$^+$ T_{eff} cells.

Moreover, in both tumour models, tiTregs appear to have some biological plasticity by presence of thymus-derived Tregs, peripheral Tregs and an inactive population of Tregs, CD25$^-$ FoxP3$^+$ T population.

Overall, the majority of frequency of tTreg clonotypes in tiTregs and the presence of pTregs represent a new view about the origin of Tregs in murine tumours, with results obtained in two different models of cancer development.

It remains to be established which types of antigens (tumour derived or self-antigens) contribute to the recruitment of these cells to the tumour site. Moreover, the function of each lineage of tiTregs in cancer immune tolerance continue unknown. The discovery of antigen specificity, function and origin of tiTregs may become a useful addition to our understanding of the relationship between cancer and the immune system, and help overcoming some of the limitations of current immunotherapy strategies.

7. References

[1] R.D. Schreiber, L.J. Old, M.J. Smyth, Cancer immunoediting: integrating immunity's roles in cancer suppression and promotion, Science 331(6024) (2011) 1565-70.

[2] D. Ribatti, The concept of immune surveillance against tumors. The first theories, Oncotarget 8(4) (2017) 7175-7180.

[3] E.J. Foley, Antigenic properties of methylcholanthrene-induced tumors in mice of the strain of origin, Cancer Res 13(12) (1953) 835-7.

[4] L.J. Old, E.A. Boyse, Immunology of Experimental Tumors, Annu Rev Med 15 (1964) 167-86.

[5] P.F. Robbins, Y. Kawakami, Human tumor antigens recognized by T cells, Curr Opin Immunol 8(5) (1996) 628-36.

[6] F.M. Burnet, The concept of immunological surveillance, Prog Exp Tumor Res 13 (1970) 1-27.

[7] O. Stutman, Tumor development after 3-methylcholanthrene in immunologically deficient athymic-nude mice, Science 183(4124) (1974) 534-6.

[8] O. Stutman, Chemical carcinogenesis in nude mice: comparison between nude mice from homozygous matings and heterozygous matings and effect of age and carcinogen dose, J Natl Cancer Inst 62(2) (1979) 353-8.

[9] G.P. Dunn, A.T. Bruce, H. Ikeda, L.J. Old, R.D. Schreiber, Cancer immunoediting: from immunosurveillance to tumor escape, Nat Immunol 3(11) (2002) 991-8.

[10] Y. Shinkai, G. Rathbun, K.P. Lam, E.M. Oltz, V. Stewart, M. Mendelsohn, J. Charron, M. Datta, F. Young, A.M. Stall, et al., RAG-2-deficient mice lack mature lymphocytes owing to inability to initiate V(D)J rearrangement, Cell 68(5) (1992) 855-67.

[11] V. Shankaran, H. Ikeda, A.T. Bruce, J.M. White, P.E. Swanson, L.J. Old, R.D. Schreiber, IFNgamma and lymphocytes prevent primary tumour development and shape tumour immunogenicity, Nature 410(6832) (2001) 1107-11.

[12] G.P. Dunn, L.J. Old, R.D. Schreiber, The three Es of cancer immunoediting, Annu Rev Immunol 22 (2004) 329-60.

[13] G.P. Dunn, L.J. Old, R.D. Schreiber, The immunobiology of cancer immunosurveillance and immunoediting, Immunity 21(2) (2004) 137-48.

[14] M.D. Vesely, M.H. Kershaw, R.D. Schreiber, M.J. Smyth, Natural innate and adaptive immunity to cancer, Annu Rev Immunol 29 (2011) 235-71.

[15] D. Mittal, M.M. Gubin, R.D. Schreiber, M.J. Smyth, New insights into cancer immunoediting and its three component phases--elimination, equilibrium and escape, Curr Opin Immunol 27 (2014) 16-25.

[16] X. Wu, M. Peng, B. Huang, H. Zhang, H. Wang, B. Huang, Z. Xue, L. Zhang, Y. Da, D. Yang, Z. Yao, R. Zhang, Immune microenvironment profiles of tumor immune equilibrium and immune escape states of mouse sarcoma, Cancer Lett 340(1) (2013) 124-33.

[17] C.M. Koebel, W. Vermi, J.B. Swann, N. Zerafa, S.J. Rodig, L.J. Old, M.J. Smyth, R.D. Schreiber, Adaptive immunity maintains occult cancer in an equilibrium state, Nature 450(7171) (2007) 903-7.

[18] C.L. Ventola, Cancer Immunotherapy, Part 1: Current Strategies and Agents, P T 42(6) (2017) 375-383.

[19] Y. Yu, J. Cui, Present and future of cancer immunotherapy: A tumor microenvironmental perspective, Oncol Lett 16(4) (2018) 4105-4113.

[20] M.A. Postow, M.K. Callahan, J.D. Wolchok, Immune Checkpoint Blockade in Cancer Therapy, J Clin Oncol 33(17) (2015) 1974-82.

[21] J. Gong, A. Chehrazi-Raffle, S. Reddi, R. Salgia, Development of PD-1 and PD-L1 inhibitors as a form of cancer immunotherapy: a comprehensive review of registration trials and future considerations, J Immunother Cancer 6(1) (2018) 8.

[22] Y. Takeuchi, H. Nishikawa, Roles of regulatory T cells in cancer immunity, Int Immunol 28(8) (2016) 401-9.

[23] P. Sharma, S. Hu-Lieskovan, J.A. Wargo, A. Ribas, Primary, Adaptive, and Acquired Resistance to Cancer Immunotherapy, Cell 168(4) (2017) 707-723.

[24] H. Zhang, J. Chen, Current status and future directions of cancer immunotherapy, J Cancer 9(10) (2018) 1773-1781.

[25] E.V. Rothenberg, Transcriptional control of early T and B cell developmental choices, Annu Rev Immunol 32 (2014) 283-321.

[26] N.R. Gascoigne, V. Rybakin, O. Acuto, J. Brzostek, TCR Signal Strength and T Cell Development, Annu Rev Cell Dev Biol 32 (2016) 327-348.

[27] R.N. Germain, T-cell development and the CD4-CD8 lineage decision, Nat Rev Immunol 2(5) (2002) 309-22.

[28] T.K. Starr, S.C. Jameson, K.A. Hogquist, Positive and negative selection of T cells, Annu Rev Immunol 21 (2003) 139-76.

[29] D.J. Laydon, C.R. Bangham, B. Asquith, Estimating T-cell repertoire diversity: limitations of classical estimators and a new approach, Philos Trans R Soc Lond B Biol Sci 370(1675) (2015).

[30] A.J. Feeney, K.D. Victor, K. Vu, B. Nadel, R.U. Chukwuocha, Influence of the V(D)J recombination mechanism on the formation of the primary T and B cell repertoires, Semin Immunol 6(3) (1994) 155-63.

[31] E.A. Motea, A.J. Berdis, Terminal deoxynucleotidyl transferase: the story of a misguided DNA polymerase, Biochim Biophys Acta 1804(5) (2010) 1151-66.

[32] D.B. Roth, V(D)J Recombination: Mechanism, Errors, and Fidelity, Microbiol Spectr 2(6) (2014).

[33] J.B. Wing, S. Sakaguchi, TCR diversity and Treg cells, sometimes more is more, Eur J Immunol 41(11) (2011) 3097-100.

[34] J. Nikolich-Zugich, M.K. Slifka, I. Messaoudi, The many important facets of T-cell repertoire diversity, Nat Rev Immunol 4(2) (2004) 123-32.

[35] S.A. Hogan, A. Courtier, P.F. Cheng, N.F. Jaberg-Bentele, S.M. Goldinger, M. Manuel, S. Perez, N. Plantier, J.F. Mouret, T.D.L. Nguyen-Kim, M.I.G. Raaijmakers, P. Kvistborg, N. Pasqual, J. Haanen, R. Dummer, M.P. Levesque, Peripheral Blood TCR Repertoire Profiling May Facilitate Patient Stratification for Immunotherapy against Melanoma, Cancer Immunol Res 7(1) (2019) 77-85.

[36] J. A.owen, J. Punt, S.A. Stranford, Kuby Immunology, 17 ed., New York, 2009.

[37] K. Fujii, T. Kanekura, Next-Generation Sequencing Technologies for Early-Stage Cutaneous T-Cell Lymphoma, Front Med (Lausanne) 6 (2019) 181.

[38] V. Golubovskaya, L. Wu, Different Subsets of T Cells, Memory, Effector Functions, and CAR-T Immunotherapy, Cancers (Basel) 8(3) (2016).

[39] P. Martinez-Sosa, L. Mendoza, The regulatory network that controls the differentiation of T lymphocytes, Biosystems 113(2) (2013) 96-103.

[40] H. Waldmann, Immunological Tolerance, Reference Module in Biomedical Sciences2014.

[41] E. Kawasaki, Type 1 diabetes and autoimmunity, Clin Pediatr Endocrinol 23(4) (2014) 99-105.

[42] R. Nurieva, J. Wang, A. Sahoo, T-cell tolerance in cancer, Immunotherapy 5(5) (2013) 513-531.

[43] M.Y. Mapara, M. Sykes, Tolerance and cancer: mechanisms of tumor evasion and strategies for breaking tolerance, J Clin Oncol 22(6) (2004) 1136-51.

[44] A. Makkouk, G.J. Weiner, Cancer immunotherapy and breaking immune tolerance: new approaches to an old challenge, Cancer Res 75(1) (2015) 5-10.

[45] M.M. Boyiadzis, M.V. Dhodapkar, R.J. Brentjens, J.N. Kochenderfer, S.S. Neelapu, M.V. Maus, D.L. Porter, D.G. Maloney, S.A. Grupp, C.L. Mackall, C.H. June, M.R. Bishop, Chimeric antigen receptor (CAR) T therapies for the treatment of hematologic malignancies: clinical perspective and significance, J Immunother Cancer 6(1) (2018) 137.

[46] Y. Xing, K.A. Hogquist, T-cell tolerance: central and peripheral, Cold Spring Harb Perspect Biol 4(6) (2012).

[47] C. Benoist, D. Mathis, Treg cells, life history, and diversity, Cold Spring Harb Perspect Biol 4(9) (2012) a007021.

[48] I.J. Huijbers, S.M. Soudja, C. Uyttenhove, M. Buferne, E.M. Inderberg-Suso, D. Colau, L. Pilotte, C.G. Powis de Tenbossche, P. Chomez, F. Brasseur, A.M. Schmitt-Verhulst, B.J. Van den Eynde, Minimal tolerance to a tumor antigen encoded by a cancer-germline gene, J Immunol 188(1) (2012) 111-21.

[49] S. Cloosen, J. Arnold, M. Thio, G.M. Bos, B. Kyewski, W.T. Germeraad, Expression of tumor-associated differentiation antigens, MUC1 glycoforms and CEA, in human thymic epithelial cells: implications for self-tolerance and tumor therapy, Cancer Res 67(8) (2007) 3919-26.

[50] R. Bonasio, M.L. Scimone, P. Schaerli, N. Grabie, A.H. Lichtman, U.H. von Andrian, Clonal deletion of thymocytes by circulating dendritic cells homing to the thymus, Nat Immunol 7(10) (2006) 1092-100.

[51] J. Oh, J.S. Shin, The Role of Dendritic Cells in Central Tolerance, Immune Netw 15(3) (2015) 111-20.

[52] H. Hadeiba, K. Lahl, A. Edalati, C. Oderup, A. Habtezion, R. Pachynski, L. Nguyen, A. Ghodsi, S. Adler, E.C. Butcher, Plasmacytoid dendritic cells transport peripheral antigens to the thymus to promote central tolerance, Immunity 36(3) (2012) 438-50.

[53] O.U. Soyer, M. Akdis, J. Ring, H. Behrendt, R. Crameri, R. Lauener, C.A. Akdis, Mechanisms of peripheral tolerance to allergens, Allergy 68(2) (2013) 161-70.

[54] D.L. Mueller, Mechanisms maintaining peripheral tolerance, Nat Immunol 11(1) (2010) 21-7.

[55] H. Nishimura, M. Nose, H. Hiai, N. Minato, T. Honjo, Development of lupus-like autoimmune diseases by disruption of the PD-1 gene encoding an ITIM motif-carrying immunoreceptor, Immunity 11(2) (1999) 141-51.

[56] E.A. Tivol, F. Borriello, A.N. Schweitzer, W.P. Lynch, J.A. Bluestone, A.H. Sharpe, Loss of CTLA-4 leads to massive lymphoproliferation and fatal multiorgan tissue destruction, revealing a critical negative regulatory role of CTLA-4, Immunity 3(5) (1995) 541-7.

[57] P. Waterhouse, J.M. Penninger, E. Timms, A. Wakeham, A. Shahinian, K.P. Lee, C.B. Thompson, H. Griesser, T.W. Mak, Lymphoproliferative disorders with early lethality in mice deficient in Ctla-4, Science 270(5238) (1995) 985-8.

[58] A. Haragan, J.K. Field, M.P.A. Davies, C. Escriu, A. Gruver, J.R. Gosney, Heterogeneity of PD-L1 expression in non-small cell lung cancer: Implications for specimen sampling in predicting treatment response, Lung Cancer 134 (2019) 79-84.

[59] S. Kleffel, C. Posch, S.R. Barthel, H. Mueller, C. Schlapbach, E. Guenova, C.P. Elco, N. Lee, V.R. Juneja, Q. Zhan, C.G. Lian, R. Thomi, W. Hoetzenecker, A. Cozzio, R. Dummer, M.C. Mihm, Jr., K.T. Flaherty, M.H. Frank, G.F. Murphy, A.H. Sharpe, T.S. Kupper, T. Schatton, Melanoma Cell-Intrinsic PD-1 Receptor Functions Promote Tumor Growth, Cell 162(6) (2015) 1242-56.

[60] P.D. Hughes, G.T. Belz, K.A. Fortner, R.C. Budd, A. Strasser, P. Bouillet, Apoptosis regulators Fas and Bim cooperate in shutdown of chronic immune responses and prevention of autoimmunity, Immunity 28(2) (2008) 197-205.

[61] A.E. Weant, R.D. Michalek, I.U. Khan, B.C. Holbrook, M.C. Willingham, J.M. Grayson, Apoptosis regulators Bim and Fas function concurrently to control autoimmunity and CD8+ T cell contraction, Immunity 28(2) (2008) 218-30.

[62] J. Hutcheson, J.C. Scatizzi, A.M. Siddiqui, G.K. Haines, 3rd, T. Wu, Q.Z. Li, L.S. Davis, C. Mohan, H. Perlman, Combined deficiency of proapoptotic regulators Bim and Fas results in the early onset of systemic autoimmunity, Immunity 28(2) (2008) 206-17.

[63] S.G. Zheng, J.H. Wang, M.N. Koss, F. Quismorio, Jr., J.D. Gray, D.A. Horwitz, CD4+ and CD8+ regulatory T cells generated ex vivo with IL-2 and TGF-beta suppress a stimulatory graft-versus-host disease with a lupus-like syndrome, J Immunol 172(3) (2004) 1531-9.

[64] W. Chen, W. Jin, N. Hardegen, K.J. Lei, L. Li, N. Marinos, G. McGrady, S.M. Wahl, Conversion of peripheral CD4+CD25- naive T cells to CD4+CD25+ regulatory T cells by TGF-beta induction of transcription factor Foxp3, J Exp Med 198(12) (2003) 1875-86.

[65] G. Deng, Tumor-infiltrating regulatory T cells: origins and features, Am J Clin Exp Immunol 7(5) (2018) 81-87.

[66] S. Sakaguchi, N. Sakaguchi, M. Asano, M. Itoh, M. Toda, Immunologic self-tolerance maintained by activated T cells expressing IL-2 receptor alpha-chains (CD25). Breakdown of a single mechanism of self-tolerance causes various autoimmune diseases, J Immunol 155(3) (1995) 1151-64.

[67] A.Y. Rudensky, Regulatory T cells and Foxp3, Immunol Rev 241(1) (2011) 260-8.

[68] C.J. Workman, A.L. Szymczak-Workman, L.W. Collison, M.R. Pillai, D.A. Vignali, The development and function of regulatory T cells, Cell Mol Life Sci 66(16) (2009) 2603-22.

[69] R. Bacchetta, F. Barzaghi, M.G. Roncarolo, From IPEX syndrome to FOXP3 mutation: a lesson on immune dysregulation, Ann N Y Acad Sci 1417(1) (2018) 5-22.

[70] T. Miyao, S. Floess, R. Setoguchi, H. Luche, H.J. Fehling, H. Waldmann, J. Huehn, S. Hori, Plasticity of Foxp3(+) T cells reflects promiscuous Foxp3 expression in conventional T cells but not reprogramming of regulatory T cells, Immunity 36(2) (2012) 262-75.

[71] X. Li, Y. Zheng, Regulatory T cell identity: formation and maintenance, Trends Immunol 36(6) (2015) 344-53.

[72] M. Najafi, B. Farhood, K. Mortezaee, Contribution of regulatory T cells to cancer: A review, J Cell Physiol 234(6) (2019) 7983-7993.

[73] M. Frydrychowicz, M. Boruczkowski, A. Kolecka-Bednarczyk, G. Dworacki, The Dual Role of Treg in Cancer, Scand J Immunol 86(6) (2017) 436-443.

[74] B. Chaudhary, E. Elkord, Regulatory T Cells in the Tumor Microenvironment and Cancer Progression: Role and Therapeutic Targeting, Vaccines (Basel) 4(3) (2016).

[75] S. Sakaguchi, T. Yamaguchi, T. Nomura, M. Ono, Regulatory T cells and immune tolerance, Cell 133(5) (2008) 775-87.

[76] S. Sakaguchi, Naturally arising CD4+ regulatory t cells for immunologic self-tolerance and negative control of immune responses, Annu Rev Immunol 22 (2004) 531-62.

[77] N. Watanabe, Y.H. Wang, H.K. Lee, T. Ito, Y.H. Wang, W. Cao, Y.J. Liu, Hassall's corpuscles instruct dendritic cells to induce CD4+CD25+ regulatory T cells in human thymus, Nature 436(7054) (2005) 1181-5.

[78] K. Atarashi, T. Tanoue, T. Shima, A. Imaoka, T. Kuwahara, Y. Momose, G. Cheng, S. Yamasaki, T. Saito, Y. Ohba, T. Taniguchi, K. Takeda, S. Hori, Ivanov, II, Y. Umesaki, K. Itoh, K. Honda, Induction of colonic regulatory T cells by indigenous Clostridium species, Science 331(6015) (2011) 337-41.

[79] H. Zeng, R. Zhang, B. Jin, L. Chen, Type 1 regulatory T cells: a new mechanism of peripheral immune tolerance, Cell Mol Immunol 12(5) (2015) 566-71.

[80] H.L. Weiner, A.P. da Cunha, F. Quintana, H. Wu, Oral tolerance, Immunol Rev 241(1) (2011) 241-59.

[81] E. Szurek, A. Cebula, L. Wojciech, M. Pietrzak, G. Rempala, P. Kisielow, L. Ignatowicz, Differences in Expression Level of Helios and Neuropilin-1 Do Not Distinguish Thymus-Derived from Extrathymically-Induced CD4+Foxp3+ Regulatory T Cells, PLoS One 10(10) (2015) e0141161.

[82] A.M. Thornton, P.E. Korty, D.Q. Tran, E.A. Wohlfert, P.E. Murray, Y. Belkaid, E.M. Shevach, Expression of Helios, an Ikaros transcription factor family member, differentiates thymic-derived from peripherally induced Foxp3+ T regulatory cells, J Immunol 184(7) (2010) 3433-41.

[83] M. Yadav, C. Louvet, D. Davini, J.M. Gardner, M. Martinez-Llordella, S. Bailey-Bucktrout, B.A. Anthony, F.M. Sverdrup, R. Head, D.J. Kuster, P. Ruminski, D. Weiss, D. Von Schack, J.A. Bluestone, Neuropilin-1 distinguishes natural and inducible regulatory T cells among regulatory T cell subsets in vivo, J Exp Med 209(10) (2012) 1713-22, S1-19.

[84] R.A. Gottschalk, E. Corse, J.P. Allison, Expression of Helios in peripherally induced Foxp3+ regulatory T cells, J Immunol 188(3) (2012) 976-80.

[85] T. Akimova, U.H. Beier, L. Wang, M.H. Levine, W.W. Hancock, Helios expression is a marker of T cell activation and proliferation, PLoS One 6(8) (2011) e24226.

[86] B. Shang, Y. Liu, S.J. Jiang, Y. Liu, Prognostic value of tumor-infiltrating FoxP3+ regulatory T cells in cancers: a systematic review and meta-analysis, Sci Rep 5 (2015) 15179.

[87] A. Facciabene, G.T. Motz, G. Coukos, T-regulatory cells: key players in tumor immune escape and angiogenesis, Cancer Res 72(9) (2012) 2162-71.

[88] Y. Zhou, N. Shao, N. Aierken, C. Xie, R. Ye, X. Qian, Z. Hu, J. Zhang, Y. Lin, Prognostic value of tumor-infiltrating Foxp3+ regulatory T cells in patients with breast cancer: a meta-analysis, J Cancer 8(19) (2017) 4098-4105.

[89] A.L. Gerber, A. Munst, C. Schlapbach, M. Shafighi, D. Kiermeir, R. Husler, R.E. Hunger, High expression of FOXP3 in primary melanoma is associated with tumour progression, Br J Dermatol 170(1) (2014) 103-9.

[90] N. Hiraoka, K. Onozato, T. Kosuge, S. Hirohashi, Prevalence of FOXP3+ regulatory T cells increases during the progression of pancreatic ductal adenocarcinoma and its premalignant lesions, Clin Cancer Res 12(18) (2006) 5423-34.

[91] D.M. Frey, R.A. Droeser, C.T. Viehl, I. Zlobec, A. Lugli, U. Zingg, D. Oertli, C. Kettelhack, L. Terracciano, L. Tornillo, High frequency of tumor-infiltrating FOXP3(+) regulatory T cells predicts improved survival in mismatch repair-proficient colorectal cancer patients, Int J Cancer 126(11) (2010) 2635-43.

[92] J. Carreras, A. Lopez-Guillermo, B.C. Fox, L. Colomo, A. Martinez, G. Roncador, E. Montserrat, E. Campo, A.H. Banham, High numbers of tumor-infiltrating FOXP3-positive regulatory T cells are associated with improved overall survival in follicular lymphoma, Blood 108(9) (2006) 2957-64.

[93] X. Wang, M. Lang, T. Zhao, X. Feng, C. Zheng, C. Huang, J. Hao, J. Dong, L. Luo, X. Li, C. Lan, W. Yu, M. Yu, S. Yang, H. Ren, Cancer-FOXP3 directly activated CCL5 to recruit FOXP3(+)Treg cells in pancreatic ductal adenocarcinoma, Oncogene 36(21) (2017) 3048-3058.

[94] A.W. Mailloux, M.R. Young, Regulatory T-cell trafficking: from thymic development to tumor-induced immune suppression, Crit Rev Immunol 30(5) (2010) 435-47.

[95] A. Dahmani, J.S. Delisle, TGF-beta in T Cell Biology: Implications for Cancer Immunotherapy, Cancers (Basel) 10(6) (2018).

[96] B. Ondondo, E. Jones, A. Godkin, A. Gallimore, Home sweet home: the tumor microenvironment as a haven for regulatory T cells, Front Immunol 4 (2013) 197.

[97] S. Sakaguchi, K. Wing, Y. Onishi, P. Prieto-Martin, T. Yamaguchi, Regulatory T cells: how do they suppress immune responses?, Int Immunol 21(10) (2009) 1105-11.

[98] B. Akkaya, Y. Oya, M. Akkaya, J. Al Souz, A.H. Holstein, O. Kamenyeva, J. Kabat, R. Matsumura, D.W. Dorward, D.D. Glass, E.M. Shevach, Regulatory T cells mediate specific suppression by depleting peptide-MHC class II from dendritic cells, Nat Immunol 20(2) (2019) 218-231.

[99] A. Chruscinski, H. Sadozai, V. Rojas-Luengas, A. Bartczak, R. Khattar, N. Selzner, G.A. Levy, Role of Regulatory T Cells (Treg) and the Treg Effector Molecule Fibrinogen-like Protein 2 in Alloimmunity and Autoimmunity, Rambam Maimonides Med J 6(3) (2015).

[100] A.E. Powell, G. Vlacich, Z.Y. Zhao, E.T. McKinley, M.K. Washington, H.C. Manning, R.J. Coffey, Inducible loss of one Apc allele in Lrig1-expressing progenitor cells results in multiple distal colonic tumors with features of familial adenomatous polyposis, Am J Physiol Gastrointest Liver Physiol 307(1) (2014) G16-23.

[101] J. Suffner, K. Hochweller, M.C. Kuhnle, X. Li, R.A. Kroczek, N. Garbi, G.J. Hammerling, Dendritic cells support homeostatic expansion of Foxp3+ regulatory T cells in Foxp3.LuciDTR mice, J Immunol 184(4) (2010) 1810-20.

[102] Y. Li, P. Kundu, S.W. Seow, C.T. de Matos, L. Aronsson, K.C. Chin, K. Karre, S. Pettersson, G. Greicius, Gut microbiota accelerate tumor growth via c-jun and STAT3 phosphorylation in APCMin/+ mice, Carcinogenesis 33(6) (2012) 1231-8.

[103] S. Kado, K. Uchida, H. Funabashi, S. Iwata, Y. Nagata, M. Ando, M. Onoue, Y. Matsuoka, M. Ohwaki, M. Morotomi, Intestinal microflora are necessary for development of spontaneous adenocarcinoma of the large intestine in T-cell receptor beta chain and p53 double-knockout mice, Cancer Res 61(6) (2001) 2395-8.

[104] S. Tomkovich, Y. Yang, K. Winglee, J. Gauthier, M. Muhlbauer, X. Sun, M. Mohamadzadeh, X. Liu, P. Martin, G.P. Wang, E. Oswald, A.A. Fodor, C. Jobin,

Locoregional Effects of Microbiota in a Preclinical Model of Colon Carcinogenesis, Cancer Res 77(10) (2017) 2620-2632.

[105] M. Harvey, M.J. McArthur, C.A. Montgomery, Jr., A. Bradley, L.A. Donehower, Genetic background alters the spectrum of tumors that develop in p53-deficient mice, FASEB J 7(10) (1993) 938-43.

[106] S. Zelenay, T. Lopes-Carvalho, I. Caramalho, M.F. Moraes-Fontes, M. Rebelo, J. Demengeot, Foxp3+ CD25- CD4 T cells constitute a reservoir of committed regulatory cells that regain CD25 expression upon homeostatic expansion, Proc Natl Acad Sci U S A 102(11) (2005) 4091-6.

[107] T. Nishioka, J. Shimizu, R. Iida, S. Yamazaki, S. Sakaguchi, CD4+CD25+Foxp3+ T cells and CD4+CD25-Foxp3+ T cells in aged mice, J Immunol 176(11) (2006) 6586-93.

[108] N. Komatsu, K. Okamoto, S. Sawa, T. Nakashima, M. Oh-hora, T. Kodama, S. Tanaka, J.A. Bluestone, H. Takayanagi, Pathogenic conversion of Foxp3+ T cells into TH17 cells in autoimmune arthritis, Nat Med 20(1) (2014) 62-8.

[109] J.D. Fontenot, M.A. Gavin, A.Y. Rudensky, Foxp3 programs the development and function of CD4+CD25+ regulatory T cells, Nat Immunol 4(4) (2003) 330-6.

[110] K. Wang, T. Shen, G.P. Siegal, S. Wei, The CD4/CD8 ratio of tumor-infiltrating lymphocytes at the tumor-host interface has prognostic value in triple-negative breast cancer, Hum Pathol 69 (2017) 110-117.

[111] W. Shah, X. Yan, L. Jing, Y. Zhou, H. Chen, Y. Wang, A reversed CD4/CD8 ratio of tumor-infiltrating lymphocytes and a high percentage of CD4(+)FOXP3(+) regulatory T cells are significantly associated with clinical outcome in squamous cell carcinoma of the cervix, Cell Mol Immunol 8(1) (2011) 59-66.

[112] D.L. Evers, C.B. Fowler, B.R. Cunningham, J.T. Mason, T.J. O'Leary, The effect of formaldehyde fixation on RNA: optimization of formaldehyde adduct removal, J Mol Diagn 13(3) (2011) 282-8.

[113] K. Vitosevic, M. Todorovic, T. Varljen, Z. Slovic, S. Matic, D. Todorovic, Effect of formalin fixation on pcr amplification of DNA isolated from healthy autopsy tissues, Acta Histochem 120(8) (2018) 780-788.

[114] V.C. Liu, L.Y. Wong, T. Jang, A.H. Shah, I. Park, X. Yang, Q. Zhang, S. Lonning, B.A. Teicher, C. Lee, Tumor evasion of the immune system by converting CD4+CD25- T cells into CD4+CD25+ T regulatory cells: role of tumor-derived TGF-beta, J Immunol 178(5) (2007) 2883-92.

[115] D. Vremec, J. Pooley, H. Hochrein, L. Wu, K. Shortman, CD4 and CD8 expression by dendritic cell subtypes in mouse thymus and spleen, J Immunol 164(6) (2000) 2978-86.

[116] M. Ahmadzadeh, A. Pasetto, L. Jia, D.C. Deniger, S. Stevanovic, P.F. Robbins, S.A. Rosenberg, Tumor-infiltrating human CD4(+) regulatory T cells display a distinct TCR repertoire and exhibit tumor and neoantigen reactivity, Sci Immunol 4(31) (2019).

[117] G. Zhou, H.I. Levitsky, Natural regulatory T cells and de novo-induced regulatory T cells contribute independently to tumor-specific tolerance, J Immunol 178(4) (2007) 2155-62.

[118] B. Valzasina, S. Piconese, C. Guiducci, M.P. Colombo, Tumor-induced expansion of regulatory T cells by conversion of CD4+CD25- lymphocytes is thymus and proliferation independent, Cancer Res 66(8) (2006) 4488-95.